Bioorganic & Medicinal Chemistry 27 (2019) 115177

Contents lists available at ScienceDirect

Bioorganic & Medicinal Chemistry

journal homepage: www.elsevier.com/locate/bmc

Exploration of zinc-binding groups for the design of inhibitors for the oxytocinase subfamily of M1 aminopeptidases

Sofia Tsoukalidou[a], Magdalini Kakou[a], Ioannis Mavridis[a], Despoina Koumantou[a], Vito Calderone[b], Marco Fragai[b], Efstratios Stratikos[a], Athanasios Papakyriakou[a,*], Dionisios Vourloumis[a,*]

[a] National Centre for Scientific Research "Demokritos", Agia Paraskevi 15310, Greece
[b] Center for Magnetic Resonance, University of Florence, Via L. Sacconi 6, 50019 Sesto Fiorentino, FI, Italy

A B S T R A C T

The oxytocinase subfamily of M1 aminopeptidases consists of three members, ERAP1, ERAP2 and IRAP that play several important biological roles, including key functions in the generation of antigenic peptides that drive human immune responses. They represent emerging targets for pharmacological manipulation of the immune system, albeit lack of selective inhibitors is hampering these efforts. Most of the previously explored small-molecule binders target the active site of the enzymes via strong interactions with the catalytic zinc(II) atom and, while achieving increased potency, they suffer in selectivity. Continuing our earlier efforts on weaker zinc(II) binding groups (ZBG), like the 3,4-diaminobenzoic acid derivatives (DABA), we herein synthesized and biochemically evaluated analogues of nine potentially weak ZBGs, based on differential substitutions of functionalized pyridinone- and pyridinethione-scaffolds, nicotinic-, isonicotinic-, aminobenzoic- and hydrazinobenzoic-acids. Crystallographic analysis of two analogues in complex with a metalloprotease (MMP-12) revealed unexpected binding topologies, consistent with the observed affinities. Our results suggest that the potency of the compounds as inhibitors of ERAP1, ERAP2 and IRAP is primarily driven by the occupation of active-site specificity pockets and their proper orientation within the enzymes.

1. Introduction

The M1 family of aminopeptidases comprises several members of high interest in pharmaceuticals, such as Aminopeptidase N,[1] or the oxytocinase subfamily of M1 aminopeptidases,[2] both emerging as important targets for drug development. The latter consists of 3 members: Endoplasmic Reticulum aminopeptidase 1 (ERAP1, also called adipose-derived leucine aminopeptidase, aminopeptidase regulator of TNFR1 shedding and endoplasmic reticulum aminopeptidase associated with antigen processing), Endoplasmic Reticulum aminopeptidase 2 (ERAP2, also called leukocyte-derived arginine aminopeptidase) and Insulin Regulated aminopeptidase (IRAP, also known as leucyl-cystinyl aminopeptidase, placental leucine aminopeptidase and oxytocinase). ERAP1 and ERAP2 are localized primarily in the ER and IRAP on the cell surface and in endosomic vesicles.[3] These three enzymes perform a variety of biological functions, although their involvement in the correct functioning of the human immune system has been extensively studied during the last decade. Accordingly, they trim antigenic peptide precursors and generate peptides that bind onto Major Histocompatibility Class I molecules for presentation to *T*-lymphocytes.[2,4] With this function, they can influence the human adaptive immune response and are emerging targets for pharmacological approaches.[5] Additional functions performed by members of this sub-family, include the regulation of blood pressure, glucose transport and peptide hormone levels, as well as roles in the innate immune responses.[6] Although several inhibitors for these enzymes have been reported in the literature, discovered either by rational design or screening approaches, a combination of shortcomings in terms of potency, pharmacology and selectivity has limited their clinical application.[5b,7] As a result, several efforts for optimizing selectivity versus potency are underway.

Based on our previous successful identification of 3,4-diaminobenzoic acid (DABA) derivatives with natural and unnatural amino acids as inhibitors of ERAP1, ERAP2 and IRAP (Fig. 1C) we examined the potential improvement of their binding affinity and/or selectivity via modification of their central scaffold, while maintaining the most successful occupants of the active-site specificity pockets (Fig. 1A, B) from our studies.[8] Firstly, in an attempt to stabilize the topology and orientation of the inhibitors in the binding site of the enzyme, we introduced ligands that could coordinate in a bidentate fashion with the metal ion.[9] Thus, a series of mono-substituted 3-hydroxypyridinone derivatives (**P1**–**P11**, Fig. 1C) were targeted, as potential bidentate Zn (II) scaffolds. Slight modification of the electronic potential of the latter, leading to an expected increase in its binding ability to the metal ion, was accomplished by the introduction of a 3-OMe group or

* Corresponding authors.
E-mail addresses: thpap@bio.demokritos.gr (A. Papakyriakou), d.vourloumis@inn.demokritos.gr (D. Vourloumis).

https://doi.org/10.1016/j.bmc.2019.115177
Received 1 July 2019; Received in revised form 11 October 2019; Accepted 17 October 2019
Available online 01 November 2019
0968-0896/

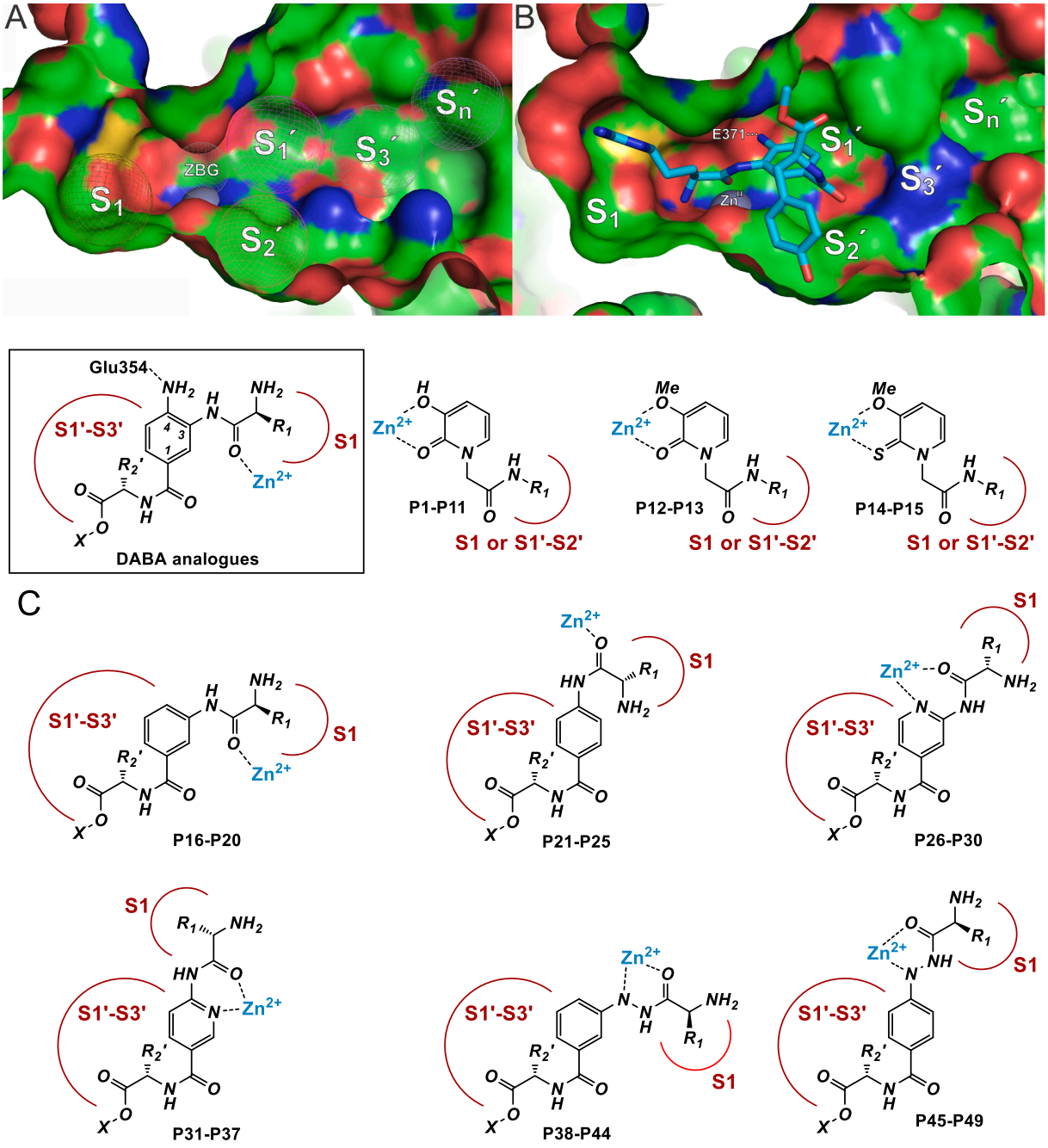

Fig. 1. A. ERAP1 topology and specificity pockets (S1, S1′, S2′, S3′, …Sn′) illustrated from a high resolution X-ray structure of ERAP1 with a bound inhibitor (PDB ID: 6Q4R).[11] **B.** Close-up view of the substrate-binding site in the crystal structure of ERAP2 bound with a DABA inhibitor (PDB ID: 5KIV),[8a] indicating the specificity subsites (S1, S1′, S2′, S3′, …Sn′) of ERAP2. The hydrogen bond formed between the N4 anilinic group of the inhibitor and the carboxylate group of Glu371 is indicated. **C.** Previously obtained diaminobenzoic acid (**DABA**) analogues and currently designed and synthesized products **P1-P49** described herein. Expected interactions with the metal ion and the occupation of active-site specificity pockets within the enzymes (ERAP1, ERAP2 and IRAP) are shown.

replacement of the carbonyl oxygen by a sulfur atom,[10] leading to analogues **P12–P13** and **P14–P15**, respectively (Fig. 1C). To assess the importance of the free aniline group in *meta*- and *para*-substituted DABAs, we synthesized a small representative library of 3-aminobenzoic acid analogues (**P16–P20**, Fig. 1C) and 4-aminobenzoic acid analogues (**P21–P25**, Fig. 1C), lacking either the 4-NH_2 or the 3-NH_2 group, respectively. Similarly, a series of NH_2-substituted isonicotinic- and nicotinic-acid derivatives were synthesized (**P26–P30** and **P31–P37**, Fig. 1C), combining the potential of a bidentate coordination with the altered electronic density of the central scaffold. Finally, an analogous bidentate chelation to the catalytic zinc ion was envisioned through the use of *meta*- and *para*-hydrazinobenzoic acid, with simultaneous one-atom extension of the S1-substitution fragment, in derivatives **P38–P44** and **P45–P49** (Fig. 1C).

Evaluation of these compounds against the three M1 aminopeptidases using an *in vitro* fluorogenic-based assay[8c] revealed moderate to low affinities, including however some low micromolar inhibitors. In addition, we obtained X-ray crystal structures of MMP-12 complexes with **P2** and **P4**, and a zinc-bound acetohydroxamic acid (AHA) inhibitor. Taken together, our results provide useful structure-activity relationships and suggest that all of the evaluated zinc-binding groups examined represent weak zinc-coordinators for this class of enzymes, allowing sidechain-subsite interactions to be the driving force in determining inhibitor efficacy.

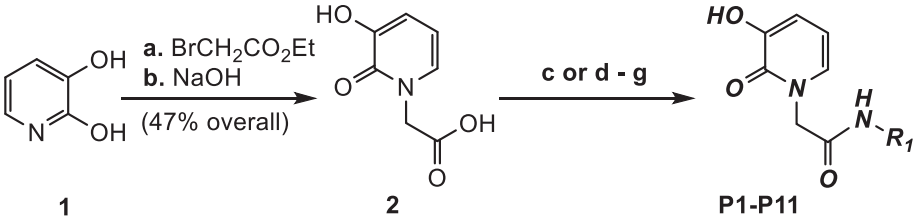

Scheme 1. Reagents and conditions: **(a)** $BrCH_2COOEt$ (5.0 equiv), reflux, 24 h, 50%; **(b)** 4 M NaOH (4.0 equiv), 25 °C, 30 min, 95%; **(c)** amine (1.1 equiv), HBTU (2.0 equiv), DIPEA (3.0 equiv), DMF (0.3–0.4 M), 60 °C, 14 h, 80% for **P1**, 43% for **P2**, 40% for **P3**, 25% for **P4**; **(d)** TFAPfp (1.3 equiv), pyridine (1.2 equiv), DMF (1.5 M), 25 °C, 1 h, 40%; **(e)** amine or protected amino acid (1.0 equiv), DIPEA (2.0–3.0 equiv), DMF (0.1–0.2 M), 25 °C, 2–18 h, 55% for **P5**, 33% for **P6**, 60% for **protected-P7**, 53% for **protected-P8**, 71% for **P9**, 84% for **P10**; **(f)** CH_2Cl_2/TFA (2/1), 25 °C, 30 min, 87% for **P7**, 79% for **P8**; **(g) P10** (1.0 equiv), H_2, Pd/C (10%), MeOH, 25 °C, 1 h, 65% for **P11**. TFAPfp = Pentafluorophenyl trifluoroacetate; HBTU = *N,N,N′,N′*-Tetramethyl-*O*-(1*H*-benzotriazol-1-yl)uronium hexafluorophosphate; DIPEA = *N,N*-Diisopropylethylamine; DMF = *N,N*-Dimethylformamide; TFA = Trifluoroacetic acid.

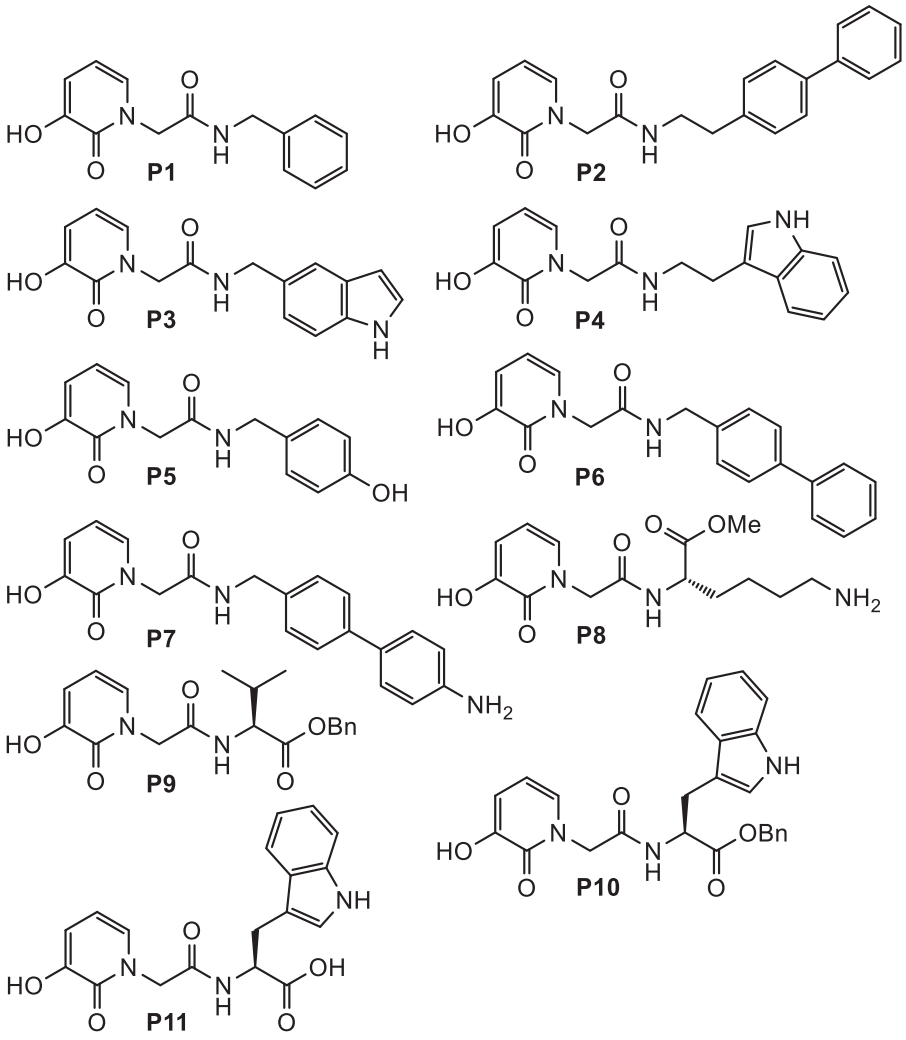

2. Results and discussion

2.1. Synthesis

Synthesis of analogues **P1–P11** commenced from the mono-alkylation of 2,3-dihydroxypyridine (**1**) with ethyl bromoacetate furnishing the corresponding adduct,[12] which was further hydrolyzed under basic conditions to produce acid **2** in 47% overall yield (Scheme 1). Coupling of the carboxylic acid moiety with various amines was envisioned by two different methods, dictated mainly by our ability to purify the desired products from the reaction mixtures. Firstly, pre-activation of the carboxylic acid with HBTU, followed by *in-situ* trapping of the activated ester with selected amines, furnished the expected products **P1–P4** in acceptable yields and purity. Alternatively, the pre-activated pentafluoro-phenyl ester (Pfp-ester) of the carboxylic acid was formed and isolated, followed, in a separate step, by its reaction with the desired protected amines and protected amino acids. Necessary deprotections (acidic and/or reductive) yielded products **P5–P11** (some products were synthesized by both methods; specific details are presented in scheme 1 and the experimental section).

Attempting to increase the electron-donating ability of the 3-oxygen, and thus the scaffold's coordinating potential to the metal center, 2,3-dihydroxypyridine (**1**) was firstly methylated through the action of dimethyl sulfate,[13] followed by its alkylation with ethyl bromoacetate furnishing ester **3**. Hydrolysis of the latter, followed by HBTU-mediated amide bond formation with selected amines, produced final products **P12-P13** (Scheme 2). Alternatively, treatment of **3** with Lawesson's reagent[14] transformed the pyridinone to the corresponding pyridinethione **4**, potentially increasing once more its binding affinity for the zinc ion. Similarly to the previous case, hydrolysis of the ester moiety and amide coupling furnishes the analogous products **P14** and **P15** for direct comparison (Scheme 2).

In order to evaluate the importance of the second aniline nitrogen, present in the previously synthesized DABA-derivatives (Fig. 1C inset), for binding, we envisioned the synthesis of a small representative library of analogues, lacking the second nitrogen either at the 4-

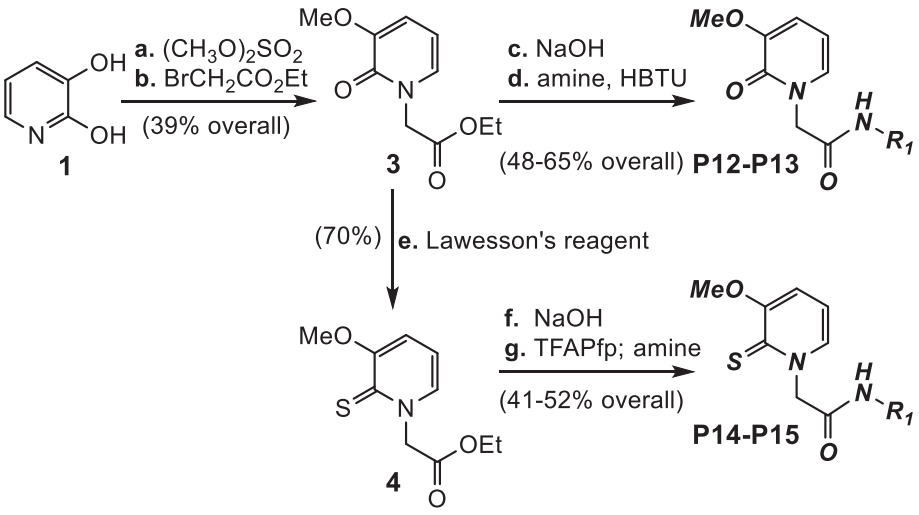

Scheme 2. Reagents and conditions: **(a)** 1.6 M NaOH (1.0 equiv), $(CH_3O)_2SO_2$ (1.1 equiv), 25 °C, 12 h, 65%; **(b)** $BrCH_2COOEt$ (1.5 equiv), K_2CO_3 (3.0 equiv), DMF (0.2 M), reflux, 18 h, 60%; **(c)** 4 M NaOH (4.0 equiv), 25 °C, 30 min, 97%; **(d)** amine (1.2–1.5 equiv), HBTU (2.0 equiv), DIPEA (3.0 equiv), DMF (0.2–0.3 M), 60 °C, 1–10 h, 50% for **P12**, 67% for **P13**; **(e)** Lawesson's reagent (0.6 equiv), toluene, reflux, 6 h, 70%; **(f)** 4 M NaOH (4.0 equiv), 25 °C, 30 min, 97%; **(g)** TFAPfp (1.5 equiv), pyridine (1.5 equiv), DMF (0.25 M), 25 °C, 18 h; then amine (2.0 equiv), DIPEA (2.0 equiv), DMF (0.2 M), 70 °C, 18 h, 42% for **P14**, 54% for **P15**.

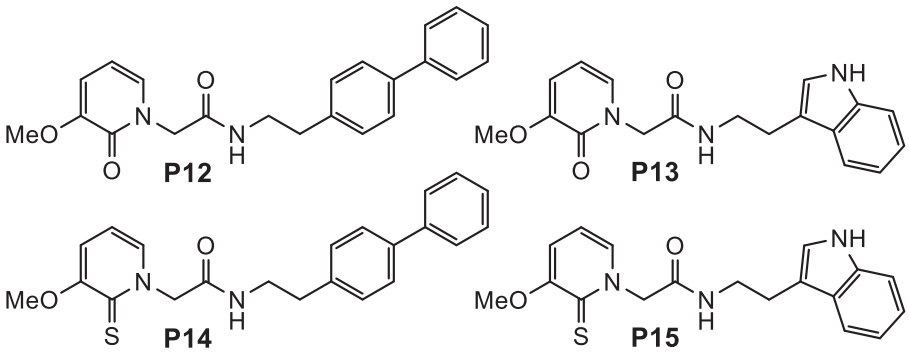

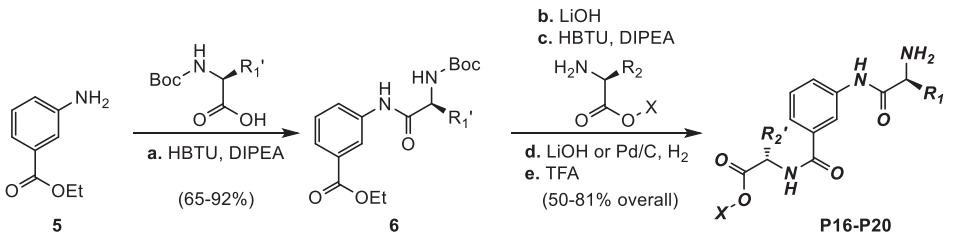

Scheme 3. Reagents and conditions: (**a**) properly protected amino acid (1.1–1.5 equiv), HBTU (2.0–3.0 equiv), DIPEA (3.0–4.0 equiv), DMF, 4–12 h, 23 °C, 65–92%; (**b**) LiOH 1 M (20 equiv), dioxane/H_2O (1:1), 3–6 h, 23 °C, 87–95%. (**c**) properly protected amino acid (1.1–1.5 equiv), HBTU (2.0–3.0 equiv), DIPEA (3.0–4.0 equiv), DMF, 4–12 h, 23 °C, 65–92%; (**d**) LiOH 1 M (20 equiv), dioxane/H_2O (1:1), 3–6 h, 23 °C, or cat. Pd/C (10% wt), H_2, MeOH, 1–2 h, 23 °C, 92–95%. (**e**) TFA/CH_2Cl_2 (1:2), 20–40 min, 23 °C, 95–98%. R_1′: side-chain of *L*-α-amino acid selected from nor-Leu, h-Phe, Arg(Z)$_2$. R_2: side-chain of *L*-α-amino acid selected from Tyr(O-tBu), Trp(OBn), Lys(Boc). R_1, R_2′: the corresponding deprotected *L*-amino acid side-chains. X: –H or –Me or –Bn.

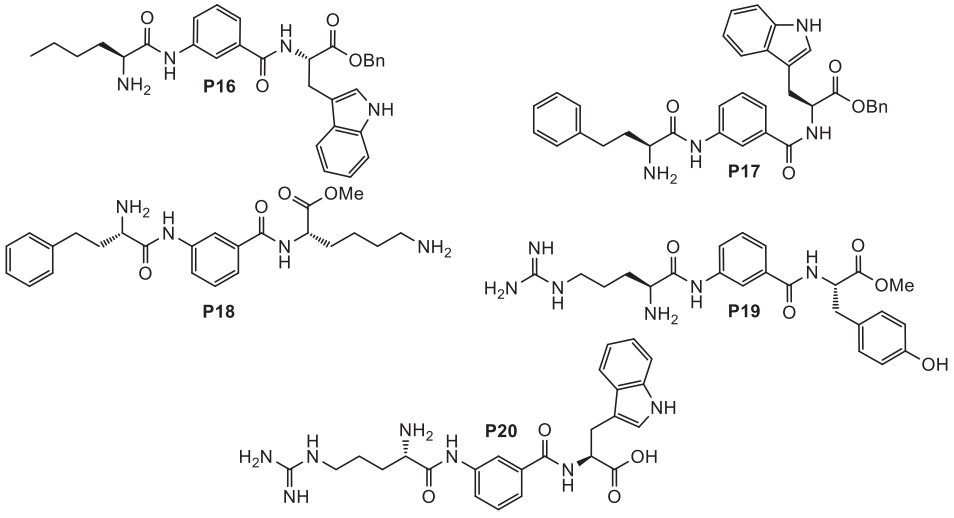

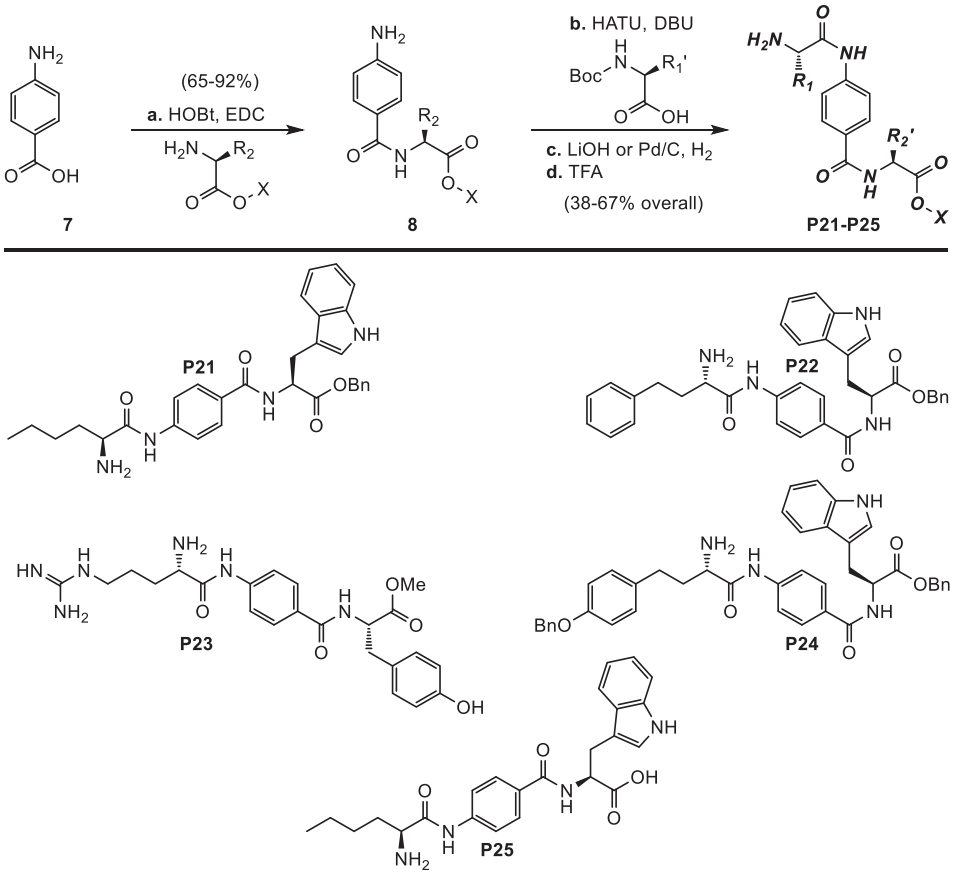

Scheme 4. Reagents and conditions: (**a**) properly protected amino acid (2.0 equiv), HOBt·H_2O (0.5 equiv), EDC·HCl (3.0 equiv), DIPEA (5.0 equiv), DMF, 12 h, 25 °C, 65–92%; (**b**) properly protected amino acid (2.0 equiv), HATU (3.0 equiv), DBU (4.0 equiv), DMF, 24–36 h, 25 °C, 45–72%; (**c**) LiOH 1 M (20 equiv), dioxane/H_2O (1:1), 3–6 h, 23 °C, or cat. Pd/C (10% wt), H_2, MeOH, 1–2 h, 25 °C, 90–95%; (**d**) TFA/CH_2Cl_2 (1:2), 20–40 min, 25 °C, 95–98%. R_1': side-chain of *L*-α-amino acid selected from nor-Leu, hPhe, Tyr(OBn), Arg(Z)$_2$. R_2: side-chain of *L*-α-amino acid selected from Tyr(O-tBu), Trp-OBn. R_1, R_2': the corresponding deprotected *L*-amino acid side-chains. X: –H or –Me or –Bn.

(**P16–P20**, Schemes 1, 3) or the 3-position (**P21–P25**, Schemes 1, 4), exploring at the same time two different orientations of the inhibitor at the active site of the enzymes. Specifically, ethyl-3-aminobenzoate (**5**) was coupled with a series of *N*-protected amino acids furnishing products **6** in high yields. Hydrolysis of the ester functionality, followed by a second amide formation, furnished, after the required deprotections, analogues **P16–P20**, as presented in Scheme 3. 4-Aminobenzoic acid (**7**) served as the starting material for the construction of the **P21–P25** analogues in a similar fashion to the 1,3-disubstituted derivatives **P16–P20** for direct comparison. The synthetic sequence is presented in Scheme 4.

Attempting to increase the zinc-biding potential of our inhibitors by introducing ligands capable of bidentate chelation, nicotinic- and isonicotinic acid scaffolds were employed. Their expected interactions at the active site of the enzyme are presented in Fig. 1 (**P26–P30** and **P31–P37**). Specifically, pre-activation of selected *N*-protected amino acids with HBTU and coupling of the reactive esters with 2-aminoisonicotinic acid (**9**) in the presence of DIPEA, furnished derivatives **10** in 65–80% isolated yields. A second amide-bond formation, followed by the required deprotections, produced final compounds **P26–P30** in good overall yields (Scheme 5).

Taking advantage of the increased reactivity of aliphatic amines over anilines in coupling reactions, HBTU-mediated reaction of 6-aminonicotinic acid (**11**) with selected carboxyl-protected amino acids produced adducts **12** in 65–80% isolated yields. A second amide formation between the anilinic nitrogen and *N*-protected amino acids, followed by the required deprotections whenever necessary, furnished analogues **P31–P37** in acceptable yields and high purity (Scheme 6).

Targeting a similar bidentate chelation to the metal center, as well as an extension of the S1-substitution by one atom, *meta*- and *para*-hydrazinobenzoic acid derivatives were enlisted for the same purpose. Thus, 3-hydrazinobenzoic acid (**13**) was coupled with selected, pre-activated with HBTU, *N*-protected amino acids furnishing adducts **14** in good yields. A second coupling reaction followed by the required deprotections produced the desired analogues **P38–P44**, as presented in Scheme 7. 1,4-disubstituted analogues were synthesized in a similar manner starting from 4-hydrazinobenzoic acid, as presented in Scheme 8, furnishing products **P45–P49** for direct comparison.

2.2. Biological activity

Biochemical evaluation of **P1–P15** against all three enzymes revealed few analogues with inhibition potential of > 50% at 100 μM, generally favoring activity for ERAP2. Initial screening was performed at a single concentration (100 μM). For all analogues with substantial inhibition at 100 μM and some inhibition at 10 μM in at least one of the enzymes, a detailed IC50 determination was performed, as presented in Table 1. Amongst our analogues, **P9** (IC_{50} 8.9 μM) and **P10** (IC_{50} 1.3 μM) exhibit the best inhibitory potential for ERAP2. Regarding their zinc-binding ability, lack of profound trends towards increased or decreased binding affinity lead us to believe that the pyridinone, its methylated analogue, or the analogous pyridinethione rings, originally selected for that purpose, do not occupy the desired position within the active site of the enzyme.

Our attempts to co-crystalize any of our analogues with either ERAP1 or ERAP2 proved unfruitful, albeit **P2** and **P4** were successfully co-crystalized with another zinc-metalloprotease (MMP-12).[15] In both X-ray structures acetohydroxamic acid (AHA), which is present as a stabilizer in the crystallization buffer, is not displaced by the ligands and is chelated to the catalytic zinc at full occupancy (Fig. 2). AHA establishes two typical hydrogen bonding interactions with the backbone of A182 and the carboxylate of the catalytic E219. The two ligands, **P2** and **P4**, do not interact with AHA and assume a similar configuration upon binding to MMP-12; their amide moiety is stabilized via two H-bonds with the backbone of Leu181 and Pro238, whereas the R_1 heterocycle is buried inside the S1′ specificity pocket of MMP-12

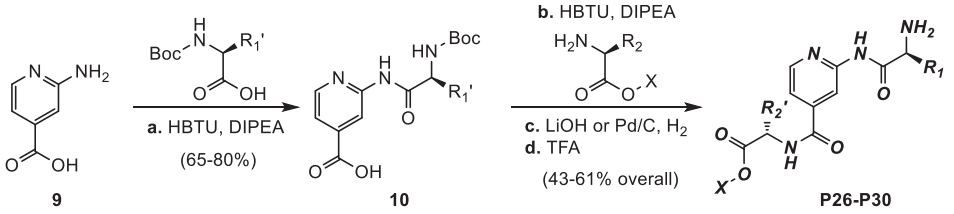

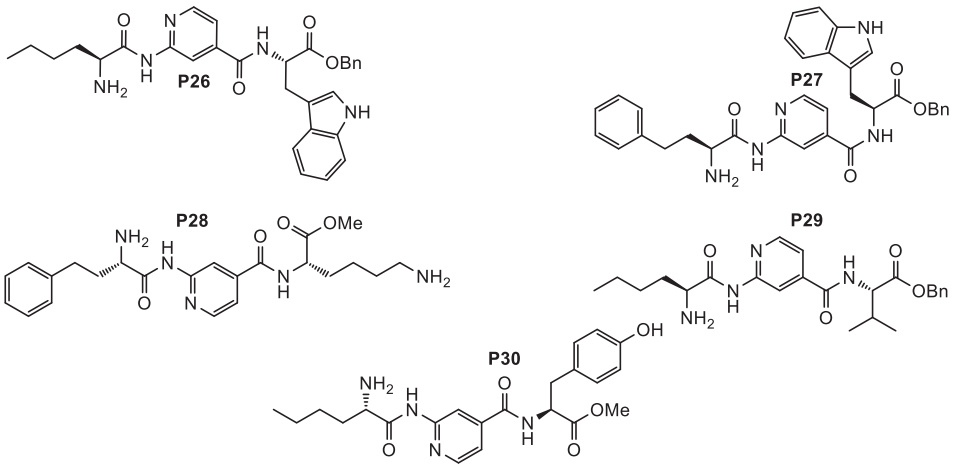

Scheme 5. Reagents and conditions: (**a**) properly protected amino acid (1.1 equiv), HBTU (2.0 equiv), DIPEA (3.0 equiv), DMF, 4–12 h, 25 °C, 65–80%; (**b**) properly protected amino acid (1.5 equiv), HBTU (3.0 equiv), DIPEA (4.0 equiv), DMF, 4–12 h, 25 °C, 50–65%; (**c**) LiOH 1 M (20 equiv), dioxane/H_2O (1:1), 3–6 h, 25 °C, or cat. Pd/C (10% wt), H_2, MeOH, 1–2 h, 25 °C, 90–95%; (**d**) TFA/CH_2Cl_2 (1:2), 20–40 min, 25 °C, 95–98%. R_1′: side-chain of *L*-α-amino acid selected from nor-Leu, hPhe. R_2: side-chain of *L*-α-amino acid selected from Val, Tyr(O-tBu), Trp-OBn, Lys(Boc). R_1, R_2′: the corresponding deprotected *L*-amino acid side-chains. X: –Me or –Bn.

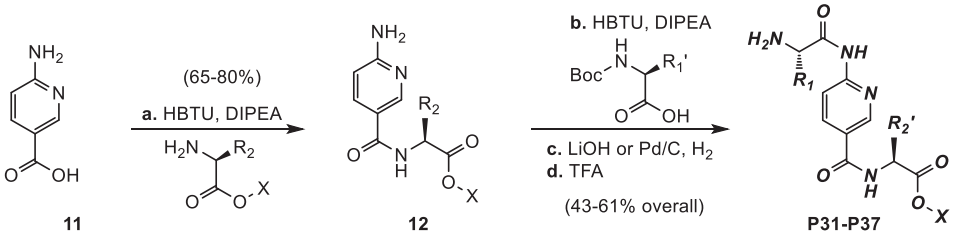

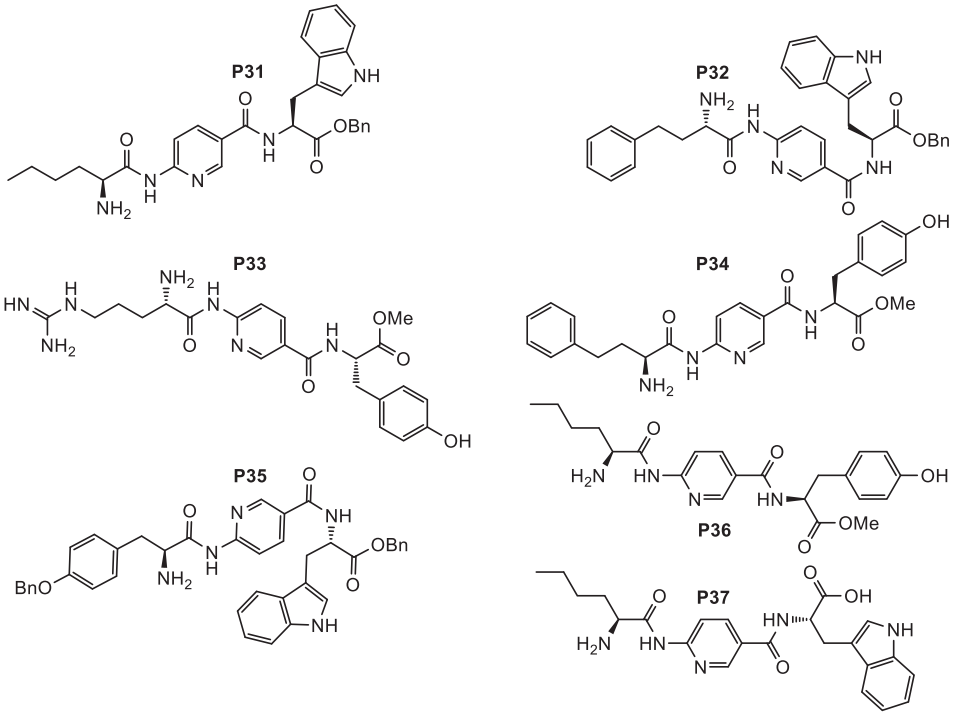

Scheme 6. Reagents and conditions: (**a**) properly protected amino acid (1.1 equiv), HBTU (3.0 equiv), DIPEA (4.0 equiv), DMF, 4–12 h, 25 °C, 65–80%; (**b**) properly protected amino acid (1.5 equiv), HBTU (3.0 equiv), DIPEA (4.0 equiv), DMF, 4–12 h, 25 °C, 50–65%; (**c**) LiOH 1 M (20 equiv), dioxane/H_2O (1:1), 3–6 h, 25 °C, or cat. Pd/C (10% wt), H_2, MeOH, 1–2 h, 25 °C, 90–95%; (**d**) TFA/CH_2Cl_2 (1:2), 20–40 min, 25 °C, 95–98%. R_1′: side-chain of *L*-α-amino acid selected from nor-Leu, hPhe, Tyr(OBn), Arg(Z)$_2$. R_2: side-chain of *L*-α-amino acid selected from Tyr(O-tBu), Trp-OBn. R_1, R_2′: the corresponding deprotected *L*-amino acid side-chains. X: –H or –Me or –Bn.

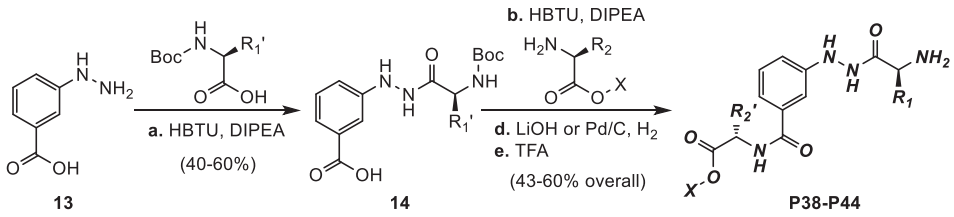

Scheme 7. Reagents and conditions: (**a**) properly protected amino acid (1.0 equiv), HBTU (1.2 equiv), DIPEA (2.0 equiv), DMF, 4–12 h, 25 °C, 40–60%; (**b**) properly protected amino acid (1.2 equiv), HBTU (2.0 equiv), DIPEA (3.0 equiv), DMF, 4–12 h, 25 °C, 50–65%; (**c**) LiOH 1 M (20 equiv), dioxane/H_2O (1:1), 3–6 h, 25 °C, or cat. Pd/C (10% wt), H_2, MeOH, 1–2 h, 25 °C, 90–95%; (**d**) TFA/CH_2Cl_2 (1:2), 20–40 min, 25 °C, 95–98%. R_1': side-chain of *L*-α-amino acid selected from nor-Leu, hPhe, Tyr(OBn), hTyr (OBn), Arg(Z)$_2$. R_2: side-chain of *L*-α-amino acid selected from Val(OBn), Tyr(O-tBu), Trp-OBn. R_1, R_2': the corresponding deprotected *L*-amino acid side-chains. X: –H or –Me or –Bn.

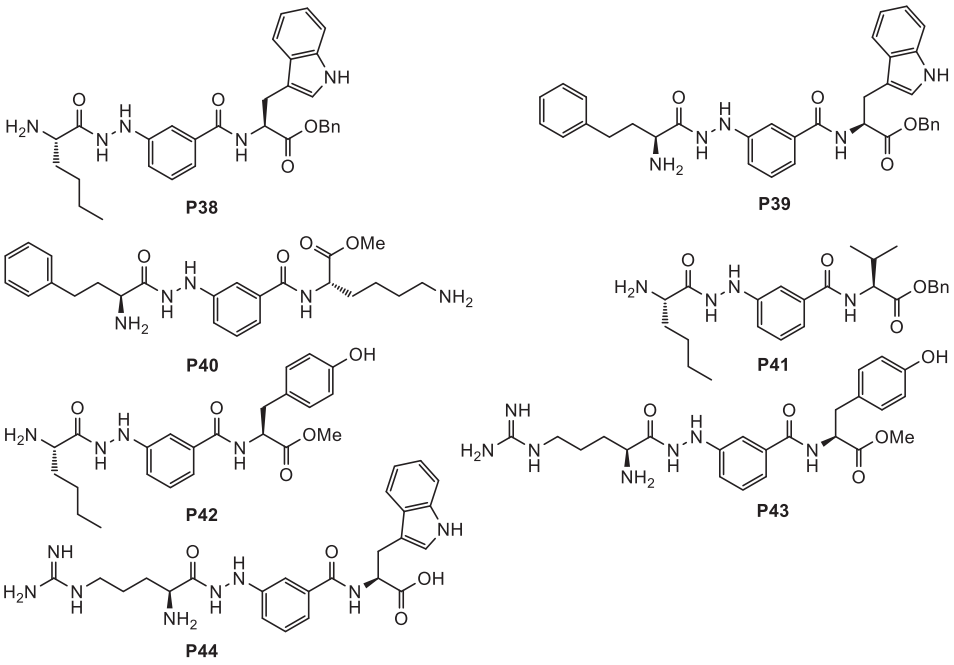

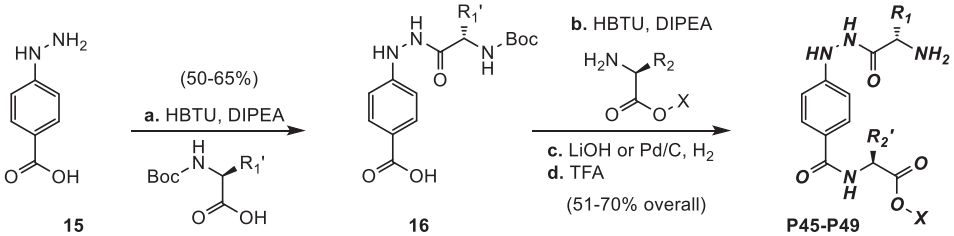

Scheme 8. Reagents and conditions: (**a**) properly protected amino acid (1.0 equiv), HBTU (1.2 equiv), DIPEA (2.0 equiv), DMF, 4–12 h, 25 °C, 50–65%; (**b**) properly protected amino acid (1.2 equiv), HBTU (2.0 equiv), DIPEA (3.0 equiv), DMF, 4–12 h, 25 °C, 60–75%; (**c**) LiOH 1 M (20 equiv), dioxane/H_2O (1:1), 3–6 h, 25 °C, or cat. Pd/C (10% wt), H_2, MeOH, 1–2 h, 25 °C, 90–95%; (**d**) TFA/CH_2Cl_2 (1:2), 20–40 min, 25 °C, 95–98%. R_1': side-chain of *L*-α-amino acid selected from nor-Leu, hPhe, Arg(Z)$_2$. R_2: side-chain of *L*-α-amino acid selected from Tyr(O-tBu), Trp-OBn. R_1, R_2': the corresponding deprotected *L*-amino acid side-chains. X: –Me or –Bn.

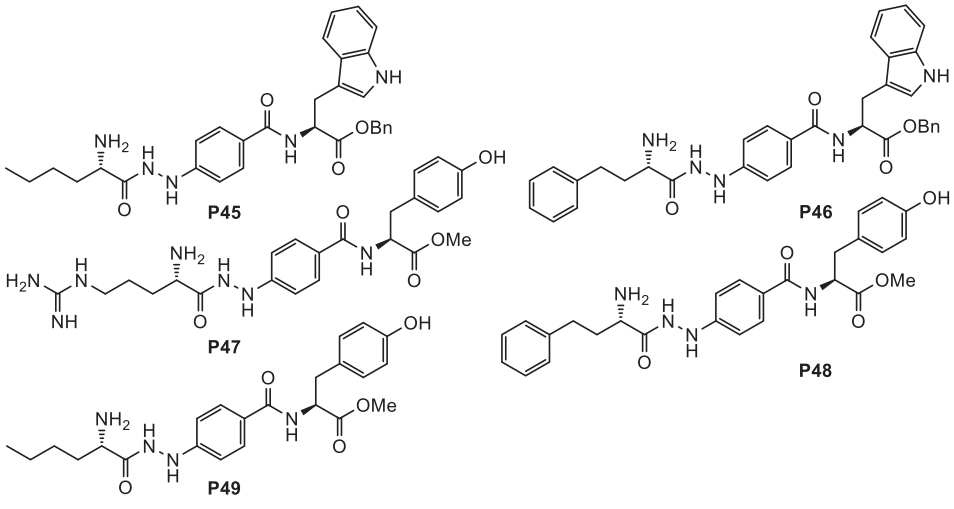

Table 1
In vitro evaluation of the designed inhibitors for ERAP1, ERAP2 and IRAP. In parenthesis, calculated K_i values for competitive inhibition.

	IC_{50}, μM (K_i, μM)		
Compound	ERAP1	ERAP2	IRAP
P2	19.1 ± 6.0 (17.5)	50.3 ± 16.2 (27.4)	24.8 ± 12.7 (13.0)
P4	–	31.3 ± 6.7 (17.7)	–
P9	48.5 ± 10.0 (44)	8.9 ± 2.4 (4.9)	33.6 ± 2.5 (17.6)
P10	20.2 ± 1.2 (18.5)	1 0.3 ± 0.6 (0.7)	10.9 ± 1.8 (5.7)
P11	–	39.3 ± 4.9 (21.4)	–
P14	25.6 ± 14.8 (23.4)	31.9 ± 10.6 (17.4)	16.7 ± 5.2 (8.7)
P16	> 100	> 10	6.2 (3.2)
P21	> 100	8.8 (4.8)	> 10
P26	> 10	> 10	8.8 (4.6)
P38	> 10	7.9 (4.3)	7.2 (3.8)
P45	11.9 (10.9)	2.2 (1.2)	2.5 (1.3)
P46	5.1 ± 0.9 (4.7)	> 10	> 10

(Fig. 2). It should be noted that the IC_{50} values for **P2** and **P4** were measured at 81 ± 8 μM and 150 ± 60 μM, respectively, therefore lack of interaction between the hydroxypyridinone and the catalytic Zn(II) is probably due to competition with the high concentration of AHA used (200 mM), as previously observed with other MMP-12 inhibitors.[16] This is also supported by the results from docking calculations of **P2** and **P4** using the X-ray structures of ligand-free MMP-12, which indicate that both compounds could bind zinc with their R_1 moiety accommodated in the S1′ pocket (Supporting Information, Fig. S1). Although direct comparison is not possible between matrix metalloproteinases and M1 aminopeptidases, our biochemical results justify our hypothesis regarding the absence of metal chelation.

3- and 4-Aminobenzoic acid disubstituted derivatives **P16-P25** were less active than the corresponding DABA analogues, more probably due to the loss of a stabilizing H-bonding interaction with the carboxylate group of Glu354 in the catalytic site of ERAP1 (equivalent to Glu371 in ERAP2, Fig. 1B). Regarding the nicotinic- and isonicotinic-based inhibitors (**P26-P37**), and assuming a similar bound configuration with the DABA inhibitor in the X-ray structure of ERAP2 (Fig. 1B), our molecular modeling calculations (Supporting Information, Fig. S2) reveal a distance of the heterocyclic N from the metal of over 5 Å. Consequently, these compounds fail to engage zinc in a bidentate fashion and thus exhibit lower affinities with respect to their DABA-based analogues. Similarly, for the hydrazinobenzoic acid derivatives **P38-P49**, the one-atom extension (acyl hydrazone *vs.* amide) probably results in a significant change in the topology and orientation of the inhibitors within the active site of the enzymes, mainly in the S2′ and the S3′ pockets, leading to an overall reduction in potency, with respect to their DABA analogues.

To confirm the hypothesized mechanism of action of the synthesized compounds we performed Micaelis-Menten analysis of compound P45 with IRAP (Fig. 3). Presence of 50% saturating concentration of **P45** affected only the K_M value and not the K_{cat} parameter, suggesting that the inhibitor is competitive. Thus, it likely occupies the catalytic site, even absent of coordinating interactions with the catalytic Zn(II) atom, in agreement with previous crystallographic analysis of a DABA homologue.[8a]

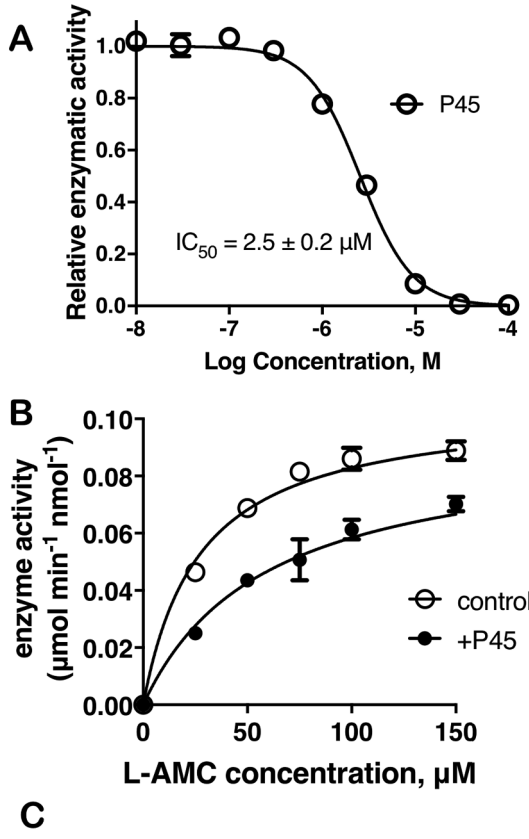

C

IRAP MM	Control	+ 2.5μM P45
K_M (μM)	27±3	59±8
K_{cat} (μmol min^{1} nmol^{1})	0.10±0.01	0.09±0.01

Fig. 3. Michaelis-Menten analysis of the effect of **P45** on the activity of IRAP using L-AMC as substrate. **A.** Titration of P**45** results in a dose-dependent inhibition of IRAP with an IC50 of 2.5μM. **B.** Michaelis-Menten curves in the absence or presence of 2.5 μM of P45. **C.** Calculated parameters from fitting the data in **B** to a standard Michaelis-Menten model.

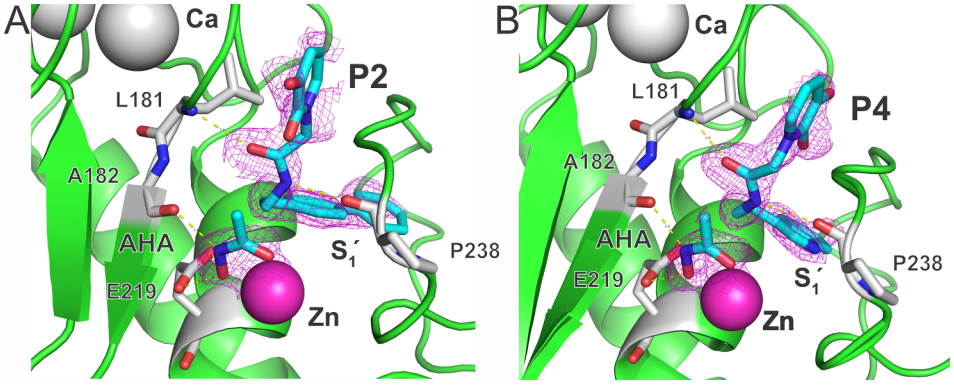

Fig. 2. Close-up view of the catalytic domain in the X-ray crystal structures of MMP-12 bound with: **(A)** acetohydroxamic acid (AHA) and **P2** (PDB ID: 6RLY), **(B)** AHA and **P4** (PDB ID: 6RD0). The electron density of the ligands is contoured at 1.0 σ, while the specificity pocket S1′, the catalytic Zn(II) and the Ca(II) ions are indicated. Yellow dashed lines indicate H-bonding interactions between the ligands and MMP-12 residues. (For interpretation of the references to colour in this figure legend, the reader is referred to the web version of this article.)

3. Conclusions

In this study we explored the efficacy of nine weakly coordinating ZBGs for the development of active-site inhibitors of the oxytocinase subfamily of M1 aminopeptidases. The pyridinone- and pyridinethione-based series (**P1-P15**) displayed low potencies, presumably due to lower affinity for the catalytic metal ion, but mostly due to their inability to occupy simultaneously the S1 and the Sn′ subsites. Crystallographic analysis of **P2** and **P4** in complex with a matrix metalloproteinase (MMP-12) revealed binding topologies with no zinc engagement (Fig. 2), consistent with their low affinities and high concentration of AHA used in the crystallization media. Removal of the free anilinic group from the DABA analogues (**P16-P25**) led to loss of stabilizing interactions within the catalytic center and significant reduction of the compounds potency. Nicotinic- and isonicotinic-based inhibitors (**P26-P37**), as well as hydrazinobenzoic acid derivatives (**P38-P49**) proved incapable to assume the required topology and orientation for an efficient bidentate coordination to the metal center and the simultaneous occupation of the specificity pockets of the enzyme. Overall, our results suggest that the potency of the compounds as inhibitors of ERAP1, ERAP2 and IRAP is primarily driven by the occupation of active-site specificity pockets, and none of the tested zinc-binding groups had sufficient affinity to properly orient the inhibitor on a canonical conformation within the active site. Future optimization of specificity pocket occupancy may lead to inhibitors that block the active site with little to no engagement of the Zn(II) atom, reducing off-target effects on other metalloproteases.

4. Experimental

4.1. General methods

Unless stated otherwise, all solvents and reagents were obtained from commercial suppliers and used without further purification. All reactions were magnetically stirred with Teflon stir bars, and temperatures were measured externally. Reactions that required anhydrous conditions were carried out in flame-dried (vacuum < 0.5 Torr) glassware under Ar atmosphere and anhydrous, freshly distilled solvents were used. All reactions were monitored by thin layer chromatography (TLC) carried out on 0.25 mm E. Merck silica gel plates (60F-254). For flash column chromatography E. Merck silica gel (60, particle size: 0.040–0.063 mm) was used. Yields refer to chromatographically and spectroscopically (^{1}H NMR) homogeneous materials. NMR spectra were recorded on a Bruker Avance DRX-500 instrument. NMR experiments were performed at 25 °C. Chemical shifts are measured in parts per million (δ) relative to the deuterated solvent used in the experiment. To designate the multiplicities the following abbreviations were designated: s, singlet; d, doublet; t, triplet; m, multiplet; b, broad.

Quantitation of the final compounds was achieved using an internal standard of 2,5-dimethylfuran (DMFu, 0.1 mM in MeOD). High resolution mass spectra (HRMS) were measured on Agilent 6224 Accurate Mass TOF LC/MS.

4.2. Synthesis of 3-Hydroxypyridinone analogues P1-P11

4.2.1. 2-(3-Hydroxy-2-oxopyridin-1(2H)-yl)-acetic acid (2)

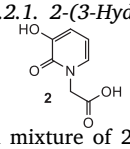

2

A mixture of 2,3-dihydroxypyridine **1** (5.5 g, 50.0 mmol, 1.0 eq) and ethyl bromoacetate (27.7 g, 250.0 mmol, 5.0 eq) was stirred under Ar atmosphere, at 25 °C, for 1 h. The mixture was then heated under reflux and stirred for 24 h. The reaction was subsequently cooled to ambient temperature and the precipitate that formed, was filtered, washed with cold acetone (3 × 3 mL) and recrystallized from warm EtOH 95%. The filtrate, which was kept separate from the washings, was concentrated, dissolved in the minimum amount of EtOH and cooled to 4 °C. The precipitate that formed was then collected by filtration and combined with the first batch. This procedure was repeated until no further precipitate could be obtained. In total the reaction yielded 3.3 g (45%) of the corresponding ester in the form of white solid: R_f = 0.7 (silica gel, 5% MeOH in CH_2Cl_2); ^{1}H NMR (500 MHz, d^6-DMSO) δ 9.11 (bs, 1H), 7.13 (dd, J = 6.8, 1.5 Hz, 1H), 6.73 (dd, J = 7.2, 1.6 Hz, 1H), 6.11 (t, J = 7.0 Hz, 1H), 4.71 (s, 2H), 4.14 (q, J = 7.1 Hz, 2H), 1.21 (t, J = 7.1 Hz, 3H) ppm; ^{13}C NMR (125 MHz, d^6-DMSO) δ 168.0, 158.1, 146.6, 128.8, 115.3, 105.1, 60.9, 50.2, 14.0 ppm.

To a stirred solution of the ester (750 mg, 3.8 mmol, 1.0 eq) in dioxane (5.0 mL, 0.7 M) was added aqueous solution of 4 M NaOH (3.8 mL, 15.2 mmol, 4.0 eq). The reaction was stirred at room temperature for 30 min and the organic solvent was evaporated under reduced pressure. The remaining aqueous phase was acidified with conc. HCl to pH 1 and extracted with AcOEt (7 × 30 mL). The combined organic extracts were dried over $MgSO_4$, filtered and evaporated, furnishing the acid **2** (610 mg, 95%) in the form of amorphous white solid. **2**: R_f = 0.8 (silica gel, 100% MeOH); ^{1}H NMR (500 MHz, CD_3OD) δ 7.06 (dd, J = 6.8, 1.4 Hz, 1H), 6.84 (dd, J = 7.3, 1.5 Hz, 1H), 6.24 (t, J = 7.1 Hz, 1H), 4.74 (s, 2H) ppm; ^{13}C NMR (125 MHz, CD_3OD) δ 170.8, 160.1, 148.1, 130.0, 117.47, 108.2, 51.7 ppm.

4.2.2. N-Benzyl-2-(3-hydroxy-2-oxopyridin-1(2H)-yl)acetamide (P1)

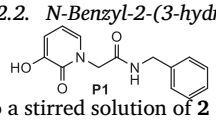

P1

To a stirred solution of **2** (190 mg, 1.1 mmol, 1.0 eq) in anhydrous DMF (1.0 mL, 1.5 M) was added pyridine (0.11 mL, 1.3 mmol, 1.2 eq) at 0 °C under an Ar atmosphere. After 5 min TFAPfp (0.25 mL, 1.5 mmol, 1.3 eq) was added and stirring was prolonged for 1 h at 25 °C. The reaction mixture was diluted with AcOEt (50 mL) and then washed with HCl 0.1 M (3 × 8 mL), 5% $NaHCO_3$ (3 × 8 mL) and brine (1 × 8 mL). The organic layer was dried over anhydrous Na_2SO_4, filtered and evaporated under reduced pressure thus furnishing the corresponding activated ester (148 mg, 40%) as an amorphous white solid.

To a mixture of benzylamine (15.3 µl, 014 mmol 1.0 eq) and DIPEA (49 µl, 0.28 mmol, 2.0 eq) in 0.5 mL of anhydrous DMF, the activated ester (48 mg, 0.14 mmol, 1.0 eq) was added dropwise as a solution in DMF (0.5 mL). The reaction was then stirred under an Ar atmosphere at 25 °C for 4 h and evaporated under reduced pressure. Addition of THF (2 mL) to the residue furnished a precipitate which was then filtered and washed with THF (3 × 0.5 mL), producing analogue **P1** (20 mg, 53%) as an amorphous white solid. **P1**: R_f = 0.5 (silica gel, 5% MeOH in CH_2Cl_2); ^{1}H NMR (500 MHz, d^6-DMSO) δ 8.99 (bs, 1H), 8.65 (t, J = 5.4 Hz, 1H), 7.41–7.18 (m, 5H), 7.10 (d, J = 6.5 Hz, 1H), 6.70 (d, J = 6.9 Hz, 1H), 6.08 (t, J = 7.0 Hz, 1H), 4.62 (s, 2H), 4.31 (d, J = 5.8 Hz, 2H) ppm; ^{13}C NMR (125 MHz, d^6-DMSO) δ 166.7, 157.9, 146.5, 139.1, 129.4, 128.2 (2C), 127.1 (2C), 126.7, 114.8, 104.6, 51.2, 42.1 ppm; HRMS calcd for $C_{14}H_{15}N_2O_3$ [$M+H^+$] 259.1083 found 259.1072.

4.2.3. N-(2-(Biphenyl-4-yl)ethyl)-2-(3-hydroxy-2-oxopyridin-1(2H)-yl) acetamide (P2)

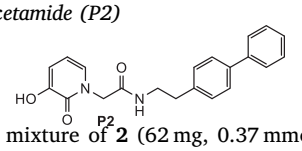

P2

A mixture of **2** (62 mg, 0.37 mmol, 1.0 eq), 2-(4-biphenyl)ethylamine (80 mg, 0.41 mmol, 1.1 eq), HBTU (281 mg, 0.74 mmol, 2.0 eq) and DIPEA (195 µl, 1.11 mmol, 3.0 eq) in anhydrous DMF (1.2 mL, 0.3 M) was stirred under an Ar atmosphere at 60 °C for 14 h. The solvent was then evaporated under reduced pressure and product **P2** (55 mg, 43%) was precipitated after addition of AcOEt (5 mL) and collected by filtration. **P2:** R_f = 0.5 (silica gel, 5% MeOH in CH_2Cl_2); ^{1}H NMR (500 MHz, d^6-DMSO) δ 9.10 (s, 1H), 8.41 (t, J = 5.3 Hz, 1H), 7.64 (d,

J = 7.4 Hz, 2H), 7.59 (d, J = 8.1 Hz, 2H), 7.46 (t, J = 7.7 Hz, 2H), 7.37–7.32 (m, 3H), 7.06 (d, J = 7.0 Hz, 1H), 6.74 (d, J = 7.5 Hz ,1H), 6.07 (t, J = 7.0 Hz, 1H), 4.57 (s, 2H), 3.34 (dd, J = 13.2, 6.8 Hz, 2H), 2.78 (t, J = 7.3 Hz, 2H) ppm; ^{13}C NMR (125 MHz, d^6-DMSO) δ 166.7, 157.9, 146.6, 140.1, 138.7, 138.1, 129.5, 129.3 (2C), 128.9 (2C), 127.2, 126.7 (2C), 126.5 (2C), 114.9, 104.7, 51.2, 40.4, 34.7 ppm; HRMS calcd for $C_{21}H_{21}N_2O_3$ [$M+H^+$] 349.1552 found 349.1541.

4.2.4. N-((1H-Indol-5-yl)methyl)-2-(3-hydroxy-2-oxopyridin-1(2H)-yl)-acetamide (P3)

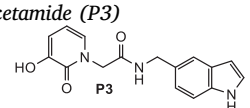

P3

It was synthesized from (1*H*-indol-5-yl)methanamine according to the procedure described for **P2**. The product (43 mg, 40%) was isolated, as an amorphous yellow solid, after precipitating it by the addition of MeOH (1 mL), filtration and washing with AcOEt (2 × 0.5 mL) and Et_2O (3 × 1 mL). **P3:** R_f = 0.7 (silica gel, 10% MeOH in AcOEt); ^{1}H NMR (500 MHz, d^6-DMSO) δ 11.02 (s, 1H), 8.96 (s, 1H), 8.56 (t, J = 5.4 Hz, 1H), 7.45 (s, 1H), 7.36–7.28 (m, 2H), 7.09 (d, J = 6.5 Hz, 1H), 7.02 (d, J = 8.3 Hz, 1H), 6.71 (d, J = 7.1 Hz, 1H), 6.38 (s, 1H), 6.08 (t, J = 7.0 Hz, 1H), 4.61 (s, 2H), 4.36 (d, J = 5.6 Hz, 2H) ppm; ^{13}C NMR (125 MHz, d^6-DMSO) δ 166.4, 157.9, 146.6, 135.0, 129.5, 129.2, 127.5, 125.6, 121.1, 118.9, 114.9, 111.2, 104.6, 100.9, 51.2, 42.8 ppm; HRMS calcd for $C_{16}H_{16}N_3O_3$ [$M+H^+$] 298.1192 found 298.1199.

4.2.5. N-(2-(1H-Indol-3-yl)ethyl)-2-(3-hydroxy-2-oxopyridin-1(2H)-yl)-acetamide (P4)

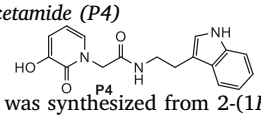

P4

It was synthesized from 2-(1*H*-indol-3-yl)ethanamine according to the procedure described for **P2**. In this case the reaction residue was purified initially by flash column chromatography (silica gel, 3% → 10% MeOH in CH_2Cl_2) and consequently by precipitation from EtOAc (2 mL) in order to afford the final product **P4** (31 mg, 25%) in the form of amorphous white solid. **P4:** R_f = 0.5 (silica gel, 5% MeOH in CH_2Cl_2); ^{1}H NMR (500 MHz, d^6-DMSO) δ 10.81 (s, 1H), 8.95 (s, 1H), 8.26 (t, J = 5.4 Hz, 1H), 7.53 (d, J = 7.8 Hz, 1H), 7.34 (d, J = 8.1 Hz, 1H), 7.17 (s, 1H), 7.09–7.03 (m, 2H), 6.98 (t, J = 7.4 Hz, 1H), 6.71 (dd, J = 7.2, 1.5 Hz, 1H), 6.07 (t, J = 7.0 Hz, 1H), 4.55 (s, 2H), 3.39–3.33 (m, 2H), 2.84 (t, J = 7.4 Hz, 2H) ppm; ^{13}C NMR (125 MHz, d^6-DMSO) δ 166.6, 157.9, 146.6, 136.2, 129.5, 127.2, 122.7, 120.9, 118.2, 118.2, 114.9, 111.6, 111.3, 104.6, 51.2, 39.7, 25.1 ppm; HRMS calcd for $C_{17}H_{18}N_3O_3$ [$M+H^+$] 312.1348 found 312.1340.

4.2.6. 2-(3-Hydroxy-2-oxopyridin-1(2H)-yl)-N-(4-hydroxybenzyl)-acetamide (P5)

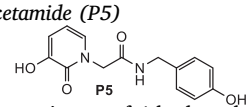

P5

To a mixture of 4-hydroxybenzylamine (20 mg, 0.16 mmol 1.1 eq) and DIPEA (26 µl, 0.15 mmol, 1.0 eq) in 0.5 mL of anhydrous DMF, the activated ester (shown for **P1**, 50 mg, 0.15 mmol, 1.0 eq) was added dropwise as a solution in DMF (0.5 mL). The reaction mixture was then stirred under an Ar atmosphere at 25 °C for 2.5 h and evaporated under reduced pressure. The product **P5** (23 mg, 55%) was isolated as amorphous white solid after the addition of THF (2 mL), filtration of the formed precipitate and washing of the solid with THF (3 × 0.5 mL). **P5:** R_f = 0.3 (silica gel, 5% MeOH in CH_2Cl_2); ^{1}H NMR (500 MHz, d^6-DMSO) δ 9.29 (s, 1H), 8.98 (s, 1H), 8.52 (t, J = 6.4 Hz, 1H), 7.08 (d, J = 7.5 Hz, 3H), 6.70 (d, J = 7.5 Hz, 3H), 6.07 (t, J = 7.5 Hz, 1H), 4.58 (s, 2H), 4.18 (d, J = 5.1 Hz, 2H) ppm; ^{13}C NMR (125 MHz, d^6-DMSO) δ 166.6, 157.9, 156.3, 146.6, 129.5, 129.2, 128.6 (2C), 115.0 (2C), 114.9, 104.7, 51.3, 41.8 ppm; HRMS calcd for $C_{14}H_{15}N_2O_4$ [$M+H^+$] 275.1032 found 275.1028.

4.2.7. N-(Biphenyl-4-ylmethyl)-2-(3-hydroxy-2-oxopyridin-1(2H)-yl)-acetamide (P6)

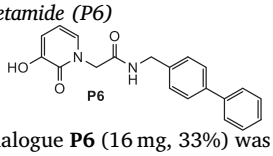

P6

Analogue **P6** (16 mg, 33%) was synthesized from 4-phenylbenzylamine according to the procedure described for **P5**. **P6**: R_f = 0.5 (silica gel, 5% MeOH in CH_2Cl_2); ^{1}H NMR (500 MHz, d^6-DMSO) δ 9.01 (s, 1H), 8.70 (t, J = 6.5 Hz, 1H), 7.64 (dd, J = 16.2, 7.9 Hz, 4H), 7.46 (t, J = 7.6 Hz, 2H), 7.34–7.39 (m, J = 17.2, 7.8 Hz, 3H), 7.11 (d, J = 5.9 Hz, 1H), 6.72 (d, J = 6.6 Hz, 1H), 6.09 (t, J = 6.6 Hz, 1H), 4.65 (s, 2H), 4.36 (d, J = 5.6 Hz, 2H) ppm; ^{13}C NMR (125 MHz, d^6-DMSO) δ 166.9, 158.0, 146.6, 140.0, 138.8, 138.4, 129.5, 128.9 (2C), 127.9 (2C), 127.3 (2C), 126.6 (2C), 115.0, 106.2, 104.7, 51.4, 41.9 ppm; HRMS calcd for $C_{20}H_{19}N_2O_3$ [$M+H^+$] 335.1396 found 335.1405.

4.2.8. N-((4′-aminobiphenyl-4-yl)methyl)-2-(3-hydroxy-2-oxopyridin-1(2H)-yl) acetamide (P7)

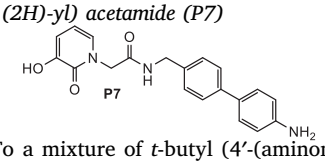

P7

To a mixture of *t*-butyl (4′-(aminomethyl)-[1,1′-biphenyl]-4-yl)-carbamate (36 mg, 0.12 mmol, 0.8 eq) and DIPEA (40 µl, 0.23 mmol, 1.5 eq) in 0.5 of anhydrous DMF, the activated ester (presented for **P1**, 50 mg, 0.15 mmol, 1.0 eq) was added dropwise as a solution in DMF (0.5 mL). The reaction was stirred under Ar atmosphere at 25 °C for 1 h, evaporated under reduced pressure and purified by column chromatography (silica gel, 6% → 10% MeOH in CH_2Cl_2). The *N*-Boc protected intermediate, isolated in the form of an amorphous white solid (40 mg, 60%, R_f = 0.6 (5% MeOH/CH_2Cl_2)), was dissolved in a mixture of CH_2Cl_2/TFA (2:1, 0.033 mM) and stirred at 25 °C for 30 min. The solution was then concentrated under reduced pressure, dissolved in a mixture of HCl 1.0 M (0.5 mL) and toluene (2 mL) and again concentrated. This procedure was repeated twice in order to afford the hydrochloride salt of **P7** (27 mg, 87%) in the form of an amorphous yellow solid. P7: ^{1}H NMR (500 MHz, d^6-DMSO) δ 8.75 (t, J = 5.7 Hz, 1H), 7.77 (d, J = 8.3 Hz, 2H), 7.63 (d, J = 8.0 Hz, 2H), 7.48 (d, J = 8.3 Hz, 2H), 7.39 (d, J = 7.9 Hz, 2H), 7.11 (d, J = 6.8 Hz, 1H), 6.72 (d, J = 7.2 Hz, 1H), 6.08 (t, J = 7.0 Hz, 1H), 4.64 (s, 2H), 4.35 (d, J = 5.6 Hz, 2H) ppm; ^{13}C NMR (125 MHz, d^6-DMSO) δ 166.9, 158.0, 146.6, 139.6, 138.9, 137.5, 131.2, 129.6, 128.0 (2C), 127.8 (2C), 126.6 (2C), 123.8 (2C), 115.0, 104.7, 51.4, 41.9 ppm; HRMS calcd for $C_{20}H_{20}N_3O_3$ [$M+H^+$] 350.1505 found 350.1500.

4.2.9. (S)-Methyl-6-amino-2-(2-(3-hydroxy-2-oxopyridin-1(2H)-yl) acetamido)-hexanoate (P8)

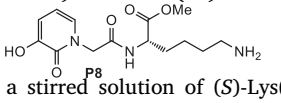

P8

To a stirred solution of (*S*)-Lys(*N*-Boc)-OMe•HCl (50 mg, 0.16 mmol, 1.1 eq) and DIPEA (65 µl, 0.37 mmol, 2.5 eq) in 0.5 mL of anhydrous DMF, was added dropwise a solution of the activated ester (presented for **P1**, 50 mg, 0.15 mmol, 1.0 eq) in 0.5 mL DMF. The reaction was then stirred under Ar atmosphere at 25 °C for 18 h and evaporated under reduced pressure. The residue was dissolvent in 40 mL CH_2Cl_2 and washed with aq. HCl 1 M (1 × 5 mL) and brine (1 × 5 mL). The organic layer was evaporated under reduced pressure and the residue was purified by column chromatography (silica gel, 4% → 10% MeOH in CH_2Cl_2). The *N*-Boc protected intermediate, isolated in the form of amorphous white solid (33 mg, 53%, R_f = 0.6 (silica gel, 5% MeOH in CH_2Cl_2)), was dissolved in a mixture of CH_2Cl_2/TFA (2:1, 0.033 mM) and stirred at 25 °C for 30 min. The solution was then concentrated under reduced pressure, dissolved in a mixture of HCl 1.0 M (0.5 mL) and toluene (2 mL) and again concentrated. This procedure was repeated twice in order to afford the hydrochloric salt of **P8** (20 mg, 79%)

in the form of an amorphous yellow solid. **P8:** ^{1}H NMR (500 MHz, CD_3OD) δ 7.15 (d, J = 6.6 Hz, 1H), 6.92 (d, J = 7.0 Hz, 1H), 6.31 (t, J = 7.1 Hz, 1H), 4.85 (s, 2H), 4.63 (d, J = 15.5 Hz, 1H), 4.55–4.49 (m, 1H), 3.73 (s, 3H), 2.94 (t, J = 7.0 Hz, 2H), 2.00–1.88 (m, 1H), 1.83–1.73 (m, 1H), 1.74–1.64 (m, 2H), 1.59–1.50 (m, 2H) ppm; ^{13}C NMR (125 MHz, CD_3OD) δ 173.5, 168.5, 158.6, 147.3, 131.4, 121.5, 111.5, 54.3, 53.5, 52.9, 40.5, 31.9, 27.8, 23.6 ppm; HRMS calcd for $C_{14}H_{22}N_3O_5$ [$M+H^+$] 312.1559 found 312.1567.

4.2.10. (S)-Benzyl 2-(2-(3-hydroxy-2-oxopyridin-1(2H)-yl)acetamido)-3-methylbutanoate (P9)

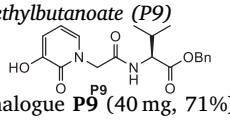

P9

Analogue **P9** (40 mg, 71%) was synthesized from (*S*)-Val-OBn•HCl according to the procedure described for **P8** and was isolated in the form of white amorphous solid. **P9:** R_f = 0.6 (silica gel, 5% MeOH in CH_2Cl_2); ^{1}H NMR (500 MHz, d^6-DMSO) δ 8.97 (s, 1H), 8.57 (d, J = 8.2 Hz, 1H), 7.41–7.32 (m, 5H), 7.05 (d, J = 6.4 Hz, 1H), 6.69 (d, J = 7.0 Hz, 1H), 6.06 (t, J = 6.9 Hz, 1H), 5.14 (q, J = 12.4 Hz, 2H), 4.67 (dd, J = 44.8, 15.7 Hz, 2H), 4.27 (t, J = 7.1 Hz, 1H), 2.11–2.04 (m, 1H), 0.88 (t, J = 7.2 Hz, 6H) ppm; ^{13}C NMR (125 MHz d^6-DMSO,) δ 170.2, 166.2, 156.9, 145.6, 134.8, 128.5, 127.5 (2C), 127.1 (2C), 127.1, 113.9, 103.6, 65.0, 56.5, 49.9, 29.3, 17.9, 17.1 ppm; HRMS calcd for $C_{19}H_{23}N_2O_5$ [$M+H^+$] 359.1607 found 359.1601.

4.2.11. (S)-Benzyl 2-(2-(3-hydroxy-2-oxopyridin-1(2H)-yl) acetamido)-3-(1H-indol-3-yl)-propanoate (P10)

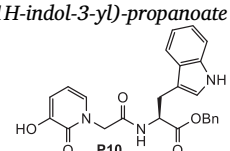

P10

Analogue **P10** (60 mg, 84%) was synthesized from (*S*)-Trp-OBn according to the procedure described for **P8** and was isolated in the form of white amorphous solid. **P10**: R_f = 0.6 (silica gel, 5% MeOH in CH_2Cl_2); ^{1}H NMR (500 MHz, CD_3OD) δ 7.50 (d, J = 7.8 Hz, 1H), 7.33 (d, J = 8.0 Hz, 1H), 7.26 (d, J = 2.1 Hz, 3H), 7.12 (d, J = 3.7 Hz, 2H), 7.09 (t, J = 7.7 Hz, 1H), 7.00 (t, J = 7.2 Hz, 2H), 6.78 (d, J = 6.9 Hz, 2H), 6.12 (t, J = 6.9 Hz, 1H), 5.00 (s, 2H), 4.80 (t, J = 6.4 Hz, 1H), 4.67–4.57 (m, 2H), 3.26 (dd, J = 15.9, 6.5 Hz, 2H) ppm; ^{13}C NMR (125 MHz, CD_3OD) δ 173.0, 169.1, 160.2, 148.2, 138.0, 136.9, 129.9, 129.5, 129.3 (2C), 129.2 (2C), 128.7, 124.8, 122.4, 119.9, 119.2, 117.2, 112.4, 110.2, 107.9, 68.1, 55.2, 52.3, 28.6 ppm; HRMS calcd for $C_{25}H_{24}N_3O_5$ [$M+H^+$] 446.1716 found 446.1704.

4.2.12. (S)-2-(2-(3-Hydroxy-2-oxopyridin-1(2H)-yl)acetamido)-3-(1H-indol-3-yl)-propanoic acid (P11)

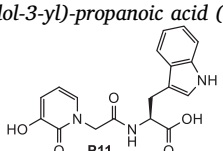

P11

Analogue **P10** (25 mg, 0.05 mmol) was dissolved in MeOH (4.0 mL, 0.0125 M) and the solution was degassed under Ar. Catalytic quantity of Pd/C 10% was added, after which Ar was replaced with H_2 and the reaction mixture was stirred for 1 h at 25 °C. The heterogeneous mixture was filtered through celite and the filtrate was concentrated under reduced pressure to afford product **P11** (13 mg, 65%) in the form of amorphous white solid. **P11:** ^{1}H NMR (500 MHz, CD_3OD) δ 7.58 (d, J = 7.8 Hz, 1H), 7.32 (d, J = 8.0 Hz, 1H), 7.13 (s, 1H), 7.08 (t, J = 7.5 Hz, 1H), 7.01 (t, J = 7.4 Hz, 1H), 6.80 (d, J = 7.0 Hz, 2H), 6.15 (t, J = 7.0 Hz, 1H), 4.73 (t, J = 5.9 Hz, 1H), 4.63 (s, 2H), 3.36 (dd, J = 14.6, 7.2 Hz 1H), 3.22 (dd, J = 14.6, 7.2 Hz, 1H) ppm; ^{13}C NMR (125 MHz, CD_3OD) δ 174.9, 168.9, 160.2, 148.2, 138.0, 129.9, 129.0, 124.7, 122.3, 119.8, 119.3, 117.2, 112.3, 110.7, 107.8, 55.0, 52.6, 28.5 ppm; HRMS calcd for $C_{18}H_{18}N_3O_5$ [$M+H^+$] 356.1246 found 356.1235.

4.3. Synthesis of 3-Methoxypyridinone analogues P12-P13.

4.3.1. Ethyl 2-(3-methoxy-2-oxopyridin-1(2H)-yl)-acetate (3)

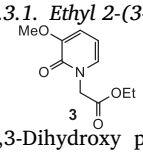

3

2,3-Dihydroxy pyridine (3.0 g, 27.0 mmol, 1.0 eq) was added to a stirred aqueous solution of NaOH 1.6 M (17 mL, 27.0 mmol, 1.0 eq) at 0 °C. After 15 min, dimethyl sulfate (3 mL, 31 mmol, 1.1 eq) was injected dropwise and stirring continued for 14 h at 25 °C. During this period the solution's pH was frequently measured and adjusted with the addition of aq. NaOH 1 M in order to prevent it from becoming overly acidic. Upon completion, the pH was adjusted to 7 and the reaction mixture was extracted with $CHCl_3$ (6 × 40 mL). The combined organic extracts were dried over anhydrous $MgSO_4$, filtered and evaporated under reduced pressure. The solid residue was recrystallized from $CHCl_3$, furnishing the corresponding ether (2.1 g, 62%) in the form of white crystals. R_f = 0.4 (5% MeOH/CH_2Cl_2); ^{1}H NMR (500 MHz, $CDCl_3$) δ 13.49 (bs, 1H), 6.95 (d, J = 6.1 Hz, 1H), 6.66 (d, J = 7.2 Hz, 1H), 6.12 (t, J = 6.9 Hz, 1H), 3.73 (s, 3H) ppm; ^{13}C NMR (125 MHz, $CDCl_3$) δ 160.2, 149.6, 125.3, 114.6, 106.3, 55.6 ppm.

To a stirred solution of the intermediate ether (250 mg, 2.0 mmol, 1.0 eq) in anhydrous DMF (10.0 mL, 0.2 M), at 25 °C under Ar atmosphere, was added K_2CO_3 (830 mg, 6.0 mmol, 3.0 eq). After 10 min, ethyl bromoacetate (0.33 mL, 3.0 mmol, 1.5 eq) was added dropwise, and the reaction mixture was heated at 100 °C for 14 h. After cooling to ambient temperature, the reaction was diluted with H_2O (30 mL) and extracted with $CHCl_3$ (60 mL). The organic layer was washed with H_2O (3 × 30 mL) and brine (1 × 40), dried with anhydrous $MgSO_4$, filtered and evaporated under reduced pressure. The residue was purified by column chromatography (50% → 80% AcOEt/CH_2Cl_2) furnishing ester **3** (250 mg, 60%) in the form of a beige amorphous solid. **3:** R_f = 0.5 (50% AcOEt/CH_2Cl_2); ^{1}H NMR (500 MHz, $CDCl_3$) δ 6.79 (d, J = 7.2 Hz, 1H), 6.53 (d, J = 7.4 Hz, 1H), 6.01 (t, J = 7.1 Hz, 1H), 4.56 (s, 2H), 4.08 (q, J = 7.1 Hz, 2H), 3.67 (s, 3H), 1.14 (t, J = 7.2 Hz, 3H) ppm; ^{13}C NMR (125 MHz, $CDCl_3$) δ 167.3, 157.6, 149.5, 128.6, 112.5, 104.5, 61.22, 55.4, 50.0, 13.7 ppm.

4.3.2. N-(2-(Biphenyl-4-yl) ethyl)-2-(3-methoxy-2-oxopyridin-1(2H)-yl)-acetamide (P12)

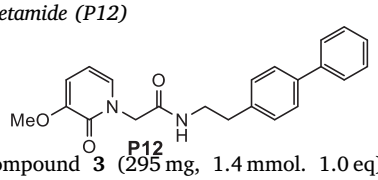

P12

Compound **3** (295 mg, 1.4 mmol. 1.0 eq) was dissolved in dioxane (5.0 mL, 0.3 M), followed by the addition of aq. NaOH 1 M (5.6 mL, 5.6 mmol, 4.0 eq). The reaction mixture was stirred at ambient temperature for 30 min and the organic solvent was evaporated under reduced pressure. The remaining aqueous solution was acidified with conc. HCl to pH = 1 and extracted with AcOEt (7 × 30 mL). The combined organic extracts were dried over anhydrous $MgSO_4$, filtered and evaporated to produce the corresponding carboxylic acid (250 mg, 97%) as amorphous white solid. R_f = 0.5 (100% MeOH); ^{1}H NMR (500 MHz, CD_3OD) δ 7.16 (dd, J = 6.9, 1.4 Hz, 1H), 6.93 (d, J = 7.5 Hz, 1H), 6.31 (dd, J = 10.2, 4.2 Hz, 1H), 4.73 (s, 2H), 3.81 (s, 3H) ppm; ^{13}C NMR (125 MHz, CD_3OD) δ 170.8, 160.0, 150.9, 130.8, 115.4, 107.2, 56.4, 51.6 ppm.

To a stirred solution of the intermediate acid (65 mg, 0.36 mmol, 1.0 eq) in anhydrous DMF (1.5 mL, 0.2 M) were added 2-(4-biphenyl) ethylamine (85 mg, 0.43 mmol, 1.2 eq), HBTU (270 mg, 0.71 mmol, 2.0 eq) and DIPEA (189 µl, 1.1 mmol, 3.0 eq), and the resulting mixture was heated to 50 °C, under Ar for 1 h. The precipitate that formed was filtrated and washed with DMF (3 × 1 mL) producing 65 mg (50%) of

analogue **P12** as amorphous white solid. **P12:** ^{1}H NMR (500 MHz, d^6-DMSO) δ 8.24 (t, J = 5.4 Hz, 1H), 7.64 (dd, J = 8.2, 1.4 Hz, 2H), 7.59 (d, J = 8.2 Hz, 2H), 7.45 (t, J = 7.7 Hz, 2H), 7.39–7.29 (m, 3H), 7.15 (dd, J = 6.9, 1.6 Hz, 1H), 6.81 (dd, J = 7.5, 1.5 Hz, 1H), 6.11 (t, J = 7.1 Hz, 1H), 4.51 (s, 2H), 3.69 (s, 3H), 3.36–3.33 (m, 2H), 2.76 (t, J = 7.3 Hz, 2H) ppm; ^{13}C NMR (125 MHz, d^6-DMSO) δ 166.7, 156.9, 149.0, 140.1, 138.64, 138.0, 130.8, 129.3 (2C), 128.9 (2C), 127.2, 126.6 (2C), 126.5 (2C), 113.4, 103.4, 55.4, 51.0, 40.3, 34.6 ppm; HRMS calcd for $C_{22}H_{23}N_2O_3$ [$M+H^+$] 363.1709 found 363.1701.

4.3.3. N-(2-(1H-Indol-3-yl)ethyl)-2-(3-methoxy-2-oxopyridin-1(2H)-yl)-acetamide (P13)

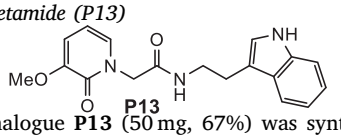

P13

Analogue **P13** (50 mg, 67%) was synthesized from 2-(1*H*-indol-3-yl)-ethanamine according to the procedure described for **P12**. An additional flash column chromatography (4% → 10 → 20% MeOH in CH_2Cl_2) was performed for high purity. **P13:** R_f = 0.3 (10% MeOH/AcOEt); ^{1}H NMR (500 MHz, CD_3OD) δ 7.53 (d, J = 7.9 Hz, 1H), 7.32 (d, J = 8.1 Hz, 1H), 7.07 (t, J = 7.5 Hz, 1H), 7.06 (s, 1H), 6.99 (t, J = 7.5 Hz, 2H), 6.85 (dd, J = 7.5, 1.2 Hz, 1H), 6.24 (t, J = 7.2 Hz, 1H), 4.57 (s, 2H), 3.75 (s, 3H), 3.48 (t, J = 7.2 Hz, 2H), 2.93 (t, J = 7.2, 2H) ppm; ^{13}C NMR (125 MHz, CD_3OD) δ 169.0, 161.0, 150.6, 138.1, 131.1, 128.7, 123.6, 122.1, 119.7, 119.2, 115.5, 113.0, 112.3, 107.2, 56.5, 53.0, 41.5, 26.0 ppm; HRMS calcd for $C_{18}H_{20}N_3O_3$ [$M+H^+$] 326.1505 found 326.1515.

4.4. Synthesis of 3-Methoxypyridinethione analogues P14-P15.

4.4.1. Ethyl 2-(3-methoxy-2-thioxopyridin-1(2H)-yl)-acetate (4)

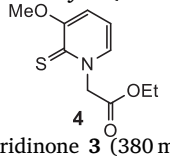

4

Pyridinone **3** (380 mg, 1.8 mmol, 1.0 eq) was dissolved in anhydrous toluene (15.0 mL, 0.12 M) under Ar, followed by the addition of Lawesson's reagent (437 mg, 1.08 mmol, 0.6 eq). The reaction mixture was heated under reflux for 6 h. Then it was allowed to cool to ambient temperature and the solvent was evaporated under reduced pressure. The residue was purified by column chromatography (60% AcOEt/CH_2Cl_2 → 100% AcOEt) furnishing intermediate **4** (295 mg, 72%) as an amorphous white solid. **4:** R_f = 0.6 (60% AcOEt/CH_2Cl_2); ^{1}H NMR (500 MHz, $CDCl_3$) δ 7.34 (dd, J = 6.6, 1.2 Hz, 1H), 6.7 (d, J = 7.9 Hz, 1H), 6.61 (t, J = 7.7, 6.7 Hz, 1H), 5.24 (s, 2H), 4.24 (q, J = 7.1 Hz, 2H), 3.90 (s, 3H), 1.27 (t, J = 7.1 Hz, 3H) ppm; ^{13}C NMR (125 MHz, $CDCl_3$) δ 172.9, 166.0, 158.5, 132.9, 111.4, 110.2, 61.5, 58.0, 56.4, 13.7 ppm.

4.4.2. N-(2-(Biphenyl-4-yl)ethyl)-2-(3-methoxy-2-thioxopyridin-1(2H)-yl)-acetamide (P14)

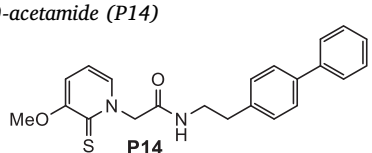

P14

Ethyl ester **4** (290 mg, 1.3 mmol, 1.0 eq) was dissolved in dioxane (6.0 mL, 0.2 M), followed by the addition of aq. NaOH 1 M (5.2 mL, 5.2 mmol, 4 eq). The reaction mixture was stirred at ambient temperature for 30 min and then the organic solvent was evaporated under reduced pressure. The remaining aqueous solution was acidified with conc. HCl to pH = 1 and extracted with AcOEt (7 × 30 mL). The combined organic extracts were dried over anhydrous $MgSO_4$ to produce the corresponding acid (245 mg, 97%) as an amorphous yellow solid. R_f = 0.3 (100% MeOH); ^{1}H NMR (500 MHz, CD_3OD) δ 7.70 (d, J = 6.6, 1H), 7.00 (d, J = 7.9 Hz, 1H), 6.79 (t, J = 7.2 Hz, 1H), 5.35 (s, 2H), 3.87 (s, 3H) ppm; ^{13}C NMR (125 MHz, CD_3OD) δ 173.8, 169.9, 159.9, 135.3, 113.4, 112.8, 59.0, 57.1 ppm.

The acid (100 mg, 0.5 mmol. 1.0 eq) was dissolved in anhydrous DMF (2.0 mL, 0.25 M) under Ar and the solution was cooled to 0 °C with stirring. Pyridine (0.08 mL, 1.0 mmol, 2 eq) was then added, followed, after 5 min, by TFAPfp (0.17 mL, 1.0 mmol, 2.0 eq). Stirring continued for 18 h at 25 °C and the mixture was then diluted with 50 mL AcOEt and filtered in order to remove the formed precipitate. The filtrate was consecutively washed with aq. HCl 0.1 M (2 × 10 mL), 5% $NaHCO_3$ (2 × 10 mL) and brine (1 × 10 mL), dried over anhydrous Na_2SO_4, filtered and evaporated under reduced pressure. The isolated activated ester was used in the next step without further purification.

A solution of the activated ester (96 mg, 0.26 mmol, 1.0 eq), 2-(4-biphenyl)ethylamine (104 mg, 0.52 mmol, 2.0 eq) and DIPEA (91 µl, 0.58 mmol, 2.0 eq) in anhydrous DMF (1.0 mL, 0.3 M) under Ar was heated to 70 °C and left to stir for 18 h. The solvent was then evaporated under reduced pressure and the residue was dissolved in AcOEt (40 mL). This solution was washed with aq. HCl 1.0 M (1 × 7 mL), saturated aq. $NaHCO_3$ (1 × 7 mL) and brine (1 × 7 mL), dried over anhydrous Na_2SO_4, filtered and evaporated under reduced pressure. Product **P14** (42 mg, 42% over two steps) was isolated after column chromatography (4% → 6% MeOH/AcOEt) as an amorphous yellow solid. **P14:** R_f = 0.4 (5% MeOH/AcOEt); ^{1}H NMR (500 MHz, $CDCl_3$) δ 7.55 (d, J = 7.8 Hz, 2H), 7.51 (d, J = 6.4 Hz, 1H), 7.46 (d, J = 8.1 Hz, 2H), 7.42 (t, J = 7.6 Hz, 2H), 7.32 (t, J = 7.3 Hz, 1H), 7.22 (d, J = 8.1 Hz, 2H), 6.69 (d, J = 7.5 Hz, 1H), 6.64 (m, 1H), 5.25 (s, 2H), 3.87 (s, 3H), 3.50 (t, J = 6.9, 2H), 2.82 (t, J = 7.1 Hz, 2H) ppm; ^{13}C NMR (125 MHz, $CDCl_3$) δ 172.3, 166.1, 159.2, 140.9, 139.3, 137.7, 132.7, 129.3 (2C), 128.8 (2C), 127.2 (2C), 127.2, 127.0 (2C), 112.5, 110.8, 59.8, 56.9, 40.8, 35.0 ppm; HRMS calcd for $C_{22}H_{23}N_2O_2S$ [$M+H^+$] 379.1480 found 379.1471.

4.4.3. N-(2-(1H-Indol-3-yl)ethyl)-2-(3-methoxy-2-thioxopyridin-1(2H)-yl)-acetamide (P15)

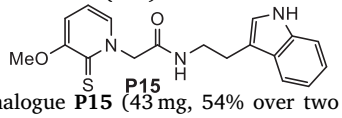

P15

Analogue **P15** (43 mg, 54% over two steps) was synthesized from 2-(1H-indol-3-yl)-ethanamine according to the procedure presented for **P14**, and isolated as an amorphous white solid. **P15:** R_f = 0.5 (5% MeOH/AcOEt); ^{1}H NMR (500 MHz, CD_3OD) δ 7.57 (ddd, J = 8.8, 7.2, 1.1 Hz, 2H), 7.32 (d, J = 8.1 Hz, 1H), 7.11 (s, 1H), 7.08 (t, J = 7.6, Hz, 1H), 6.99 (t, J = 7.4 Hz, 2H), 6.72 (dd, J = 7.8, 6.7 Hz, 1H), 5.23 (s, 2H), 3.84 (s, 3H), 3.51 (t, J = 7.2 Hz, 2H), 2.97 (t, J = 7.1 Hz, 2H) ppm; ^{13}C NMR (125 MHz, CD_3OD) δ 173.6, 168.2, 159.8, 138.1, 135.7, 128.8, 123.7, 122.3, 119.6, 119.3, 113.3, 113.1 112.8, 112.2, 60.2, 57.0, 41.6, 26.1 ppm; HRMS calcd for $C_{18}H_{20}N_3O_2S$ [$M+H^+$] 342.1276 found 342.1263.

4.5. Synthesis of analogues P16-P20

4.5.1. General procedure for the HBTU-mediated amide coupling. Synthesis of intermediates 6

A mixture of aniline **5** (1.0 eq), the appropriately protected amino acid (1.1–1.5 eq), HBTU (2.0–3.0 eq) and DIPEA (3.0–4.0 eq) in anhydrous DMF (0.25 M) was stirred under an Ar atmosphere at ambient temperature for 4–12 h. The mixture was then diluted with EtOAc and sequentially washed with HCl (1.0 M), saturated $NaHCO_3$ and brine. The organic layer was dried over anhydrous Na_2SO_4, filtered and evaporated under reduced pressure and the resulting residue was purified by column chromatography (silica gel, EtOAc/Hexanes 20% → 50%) to furnish intermediates **6** in 65–92% isolated yields.

4.5.2. General procedure for the LiOH-mediated ester hydrolysis

The corresponding ester was dissolved in a 1:1 mixture of dioxane / aq. LiOH 1.0 M (20 eq) under vigorous stirring at ambient temperature. After 3–6 h brine was added to the reaction mixture and the organic

solvent was removed under reduced pressure. The aqueous solution (pH = 12) was washed once with EtOAc and acidified by the addition of HCl 1.0 M to pH = 2. Subsequently, the aqueous layer was extracted with EtOAc (×3) and the combined organic extracts were dried over anhydrous Mg_2SO_4, filtered and concentrated under reduced pressure. The corresponding acids obtained (87–95% yields) were used without the need for further purification (> 95% purity according to NMR data).

4.5.3. General procedure for the hydrogenolysis of benzylic esters and carbamates

The corresponding ester or carbamate was dissolved in MeOH (0.025 M) and the solution was degassed under Ar. Catalytic quantity of Pd/C 10% was added, after which Ar was replaced with H_2 and the reaction mixture was stirred for 1–2 h at 25 °C. The heterogeneous mixture was filtered through celite and the filtrate was concentrated under reduced pressure to afford the desired products in excellent yields (90–95%) and purities.

4.5.4. General procedure for the acidic hydrolysis of tert-Butyl ethers and carbamates

The corresponding intermediate was dissolved in a mixture of CH_2Cl_2/TFA (2:1, 0.033 M) and the solution was stirred at ambient temperature for 20–40 min. The solvent was then evaporated to dryness under reduced pressure. The residue was dissolved in a mixture of HCl 1.0 M (0.5 mL) and toluene (2 mL) and the solution was concentrated under reduced pressure. The latter was repeated 2–3 times to ensure complete conversion of the product to the hydrochloride salt. Final analogues were isolated in excellent yields (95–99%) and purities.

4.5.4.1. (S)-Benzyl 2-(3-((S)-2-aminohexanamido)benzamido)-3-(1H-indol-3-yl)-propanoate (P16).

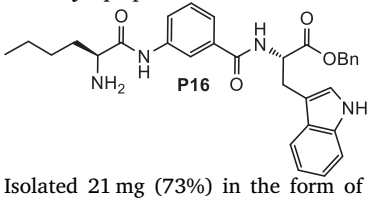

Isolated 21 mg (73%) in the form of yellow oil. ^{1}H NMR (500 MHz, CD_3OD) δ 8.07 (s, 1H), 7.76 (d, J = 8.0 Hz, 1H), 7.54 (d, J = 7.8 Hz, 1H), 7.48 (d, J = 7.7 Hz, 1H), 7.39–7.31 (m, 2H), 7.28–7.20 (m, 3H), 7.18–7.12 (m, 2H), 7.11–7.03 (m, 2H), 6.98 (t, J = 7.4 Hz, 1H), 5.06 (s, 2H), 4.98–4.92 (m, 1H), 4.09 (t, J = 6.3 Hz, 1H), 3.43 (dd, J = 14.5, 6.2 Hz, 1H), 3.37–3.32 (m, 1H), 2.03–1.87 (m, 2H), 1.50–1.34 (m, 4H), 0.92 (t, J = 7.1 Hz, 3H) ppm; ^{13}C NMR (125 MHz, CD_3OD) δ 173.4, 169.8, 168.9, 139.2, 138.0, 136.9, 136.0, 130.2, 129.4, 129.4, 129.1, 129.1, 129.0, 128.6, 124.6, 124.5, 124.3, 122.4, 120.3, 119.9, 119.1, 112.4, 110.6, 68.0, 55.8, 55.2, 32.4, 28.3, 27.9, 23.3, 14.1 ppm; HRMS calcd for $C_{31}H_{35}N_4O_4$ [$M+H^+$] 527.2658 found 527.2667.

4.5.4.2. (S)-Benzyl 2-(3-((S)-2-amino-4-phenylbutanamido)benzamido)-3-(1H-indol-3-yl)-propanoate (P17).

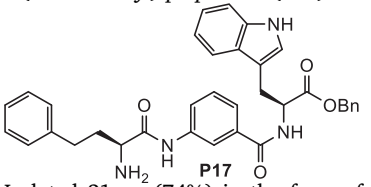

Isolated 21 mg (74%) in the form of yellow oil. ^{1}H NMR (500 MHz, CD_3OD) δ 8.03 (s, 1H), 7.72 (d, J = 7.9 Hz, 1H), 7.54 (d, J = 7.9 Hz, 1H), 7.48 (d, J = 7.7 Hz, 1H), 7.39–7.30 (m, 2H), 7.27–7.12 (m, 10*H*), 7.06 (t, J = 7.5 Hz, 1H), 7.03 (s, 1H), 6.98 (t, J = 7.4 Hz, 1H), 5.07 (s, 2H), 4.95 (t, J = 6.9 Hz, 1H), 4.12 (t, J = 6.3 Hz, 1H), 3.43 (dd, J = 14.6, 6.3 Hz, 1H), 3.37–3.32 (m, 1H), 2.81–2.69 (m, 2H), 2.31–2.17 (m, 2H) ppm; ^{13}C NMR (125 MHz, CD_3OD) δ 173.4, 169.8, 168.5, 141.1, 139.2, 138.0, 137.0, 136.1, 130.2, 129.7, 129.7, 129.7, 129.4, 129.4, 129.2, 129.2, 129.2, 129.1, 129.1, 128.7, 127.5, 124.5, 124.4, 122.5, 120.5, 119.9, 119.2, 112.4, 110.7, 68.0, 55.8, 55.1, 34.5, 32.0, 28.3 ppm; HRMS calcd for $C_{35}H_{35}N_4O_4$ [$M+H^+$] 575.2658 found 575.2648.

4.5.4.3. (S)-Methyl 6-amino-2-(3-((S)-2-amino-4-phenylbutanamido) benzamido)-hexanoate (P18).

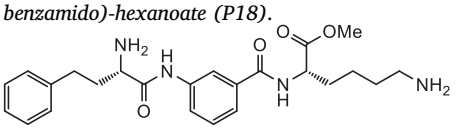

Isolated 16 mg (70%) in the form of yellow oil. ^{1}H NMR (500 MHz, CD_3OD) δ 8.11 (s, 1H), 7.78 (d, J = 7.8 Hz, 1H), 7.64 (d, J = 7.5 Hz, 1H), 7.46 (t, J = 7.9 Hz, 1H), 7.29–7.18 (m, 4H), 7.17 (t, J = 7.1 Hz, 1H), 4.62 (dd, J = 9.3, 5.1 Hz, 1H), 4.16 (t, J = 5.8 Hz, 1H), 3.75 (s, 3H), 2.94 (t, J = 7.2 Hz, 2H), 2.78 (t, J = 8.1 Hz, 2H), 2.34–2.20 (m, 2H), 2.05–1.82 (m, 2H), 1.76–1.68 (m, 2H), 1.61–1.43 (m, 2H) ppm; ^{13}C NMR (125 MHz, CD_3OD) δ 174.0, 170.1, 168.7, 141.2, 139.3, 136.1, 130.3, 129.7, 129.7, 129.3, 129.3, 127.5, 124.6, 124.6, 120.5, 55.1, 54.2, 52.8, 40.5, 34.6, 32.0, 31.7, 28.0, 24.1 ppm; HRMS calcd for $C_{24}H_{33}N_4O_4$ [$M+H^+$] 441.2502 found 441.2491.

4.5.4.4. (S)-Methyl 2-(3-((S)-2-amino-5-guanidinopentanamido)benzamido)-3-(4-hydroxyphenyl)-propanoate (P19).

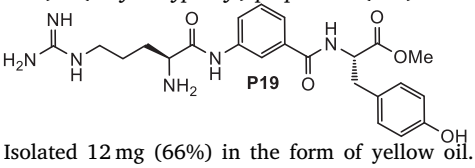

Isolated 12 mg (66%) in the form of yellow oil. ^{1}H NMR (500 MHz, CD_3OD) δ 8.06 (s, 1H), 7.79 (d, J = 7.0 Hz, 1H), 7.50 (d, J = 7.0 Hz, 1H), 7.44–7.36 (m, 1H), 7.08 (d, J = 8.3 Hz, 2H), 6.72 (d, J = 8.3 Hz, 2H), 4.76 (dd, J = 9.1, 5.5 Hz, 1H), 4.25–4.17 (m, 1H), 3.71 (s, 3H), 3.30–3.27 (m, 2H), 3.18 (dd, J = 13.9, 5.4 Hz, 1H), 3.04 (dd, J = 13.7, 9.4 Hz, 1H), 2.14–1.96 (m, 2H), 1.86–1.73 (m, 2H) ppm; ^{13}C NMR (125 MHz, CD_3OD) δ 173.7, 169.8, 168.5, 158.6, 157.3, 139.2, 136.0, 131.2, 131.2, 130.2, 129.0, 124.5, 124.5, 120.3, 116.3, 116.3, 56.2, 54.6, 52.8, 41.7, 37.3, 29.8, 25.5 ppm; HRMS calcd for $C_{23}H_{31}N_6O_5$ [$M+H^+$] 471.2356 found 471.2361.

4.5.4.5. (S)-2-(3-((S)-2-Amino-5-guanidinopentanamido)benzamido)-3-(1H-indol-3-yl)-propanoic acid (P20).

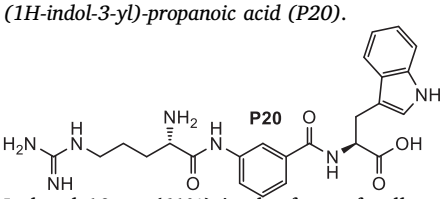

Isolated 10 mg (61%) in the form of yellow oil. ^{1}H NMR (500 MHz, CD_3OD) δ 8.04 (s, 1H), 7.77 (d, J = 7.8 Hz, 1H), 7.59 (d, J = 7.8 Hz, 1H), 7.45 (d, J = 7.7 Hz, 1H), 7.40–7.32 (m, 2H), 7.17 (s, 1H), 7.07 (t, J = 7.5 Hz, 1H), 6.98 (t, J = 7.3 Hz, 1H), 4.91 (dd, J = 8.2, 4.9 Hz, 1H), 4.20–4.12 (m, 1H), 3.49 (dd, J = 14.7, 4.8 Hz, 1H), 3.37–3.33 (m, 1H), 3.30–3.24 (m, 2H), 2.12–1.96 (m, 2H), 1.85–1.69 (m, 2H) ppm; ^{13}C NMR (125 MHz, CD_3OD) δ 175.3, 169.8, 168.5, 158.4, 139.2, 137.9, 136.1, 130.2, 128.7, 124.5, 124.3, 122.4, 120.2, 119.8, 119.2, 119.1, 112.4, 111.0, 55.6, 54.6, 41.7, 29.8, 28.2, 25.5 ppm; HRMS calcd for $C_{24}H_{30}N_7O_4$ [$M+H^+$] 480.2359 found 480.2351.

4.6. Synthesis of analogues P21-P25

4.6.1. General procedure for the HOBt/EDC-mediated amide coupling. Synthesis of intermediates 8

A solution of aniline **7** (1.0 eq), the appropriately protected amino acid (2.0 eq), HOBt·H_2O (0.5 eq), EDC·HCl (3.0 eq) and DIPEA (5.0 eq) in anhydrous DMF (0.25 M) was stirred under Ar at 25 °C for 12 h. The reaction mixture was then diluted with EtOAc and consecutively washed with HCl 1.0 M, saturated $NaHCO_3$ and brine. The organic layer was dried over anhydrous Na_2SO_4, filtered and evaporated under reduced pressure. The residue was purified by column chromatography in order to furnish intermediates **8** in 65–92% yields.

4.6.2. General procedure for the HATU/BTU-mediated amide coupling. Synthesis of analogues P21-P25

A solution of intermediates **8** (1.0 eq), a properly protected amino acid (2.0 eq), HATU (3.0 eq) and DBU (4.0 eq) in anhydrous DMF (0.25 M) was stirred under Ar at 25 °C for 24–36 h. The reaction mixture was then diluted with EtOAc and consecutively washed with HCl 1.0 M, saturated $NaHCO_3$ and brine. The organic layer was dried over anhydrous Na_2SO_4, filtered and evaporated under reduced pressure. The resulting residue was purified by column chromatography (silica gel, EtOAc/Hexanes 20% → 50%) to produce the desired intermediates in 45–72% yields. Final deprotections were performed as needed similarly to the ones described for analogues **P16**-**P20**.

4.6.2.1. (S)-Benzyl 2-(4-((S)-2-aminohexanamido)benzamido)-3-(1H-indol-3-yl)-propanoate (P21).

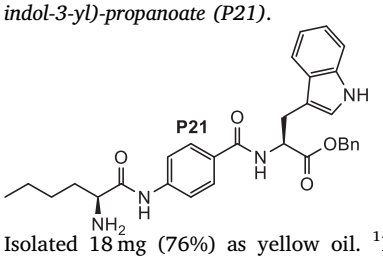

Isolated 18 mg (76%) as yellow oil. ^{1}H NMR (500 MHz, CD_3OD) δ 7.76–7.63 (m, 4H), 7.55 (d, J = 7.9 Hz, 1H), 7.34 (d, J = 8.0 Hz, 1H), 7.30–7.22 (m, 3H), 7.21–7.14 (m, 2H), 7.09 (t, J = 7.5 Hz, 1H), 7.03 (s, 1H), 6.99 (t, J = 7.5 Hz, 1H), 5.09 (s, 2H), 4.96–4.92 (m, 1H), 3.77–3.70 (m, 1H), 3.47–3.38 (m, 1H), 3.38–3.33 (m, 1H), 1.89–1.68 (m, 2H), 1.44–1.30 (m, 4H), 1.15–1.08 (m, 3H) ppm; ^{13}C NMR (125 MHz, CD_3OD) δ 173.6, 172.9, 169.5, 142.7, 138.1, 137.1, 130.6, 129.5, 128.7, 124.6, 124.4, 122.6, 122.4, 120.4, 120.0, 119.8, 119.2, 112.4, 110.8, 68.0, 56.1, 55.8, 34.4, 28.5, 28.3, 23.5, 14.1 ppm; HRMS calcd for $C_{31}H_{35}N_4O_4$ [$M+H^+$] 527.2658 found 527.2644.

4.6.2.2. (S)-Benzyl 2-(4-((S)-2-amino-4-phenylbutanamido)benzamido)-3-(1H-indol-3-yl)-propanoate (P22).

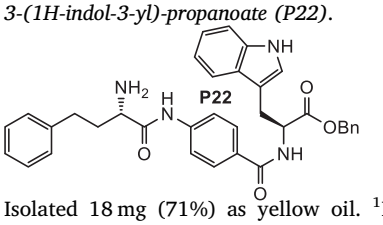

Isolated 18 mg (71%) as yellow oil. ^{1}H NMR (500 MHz, CD_3OD) δ 7.76–7.66 (m, 4H), 7.55 (d, J = 7.9 Hz, 1H), 7.34 (d, J = 7.9 Hz, 1H), 7.29–7.19 (m, 7H), 7.19–7.14 (m, 3H), 7.08 (t, J = 7.6 Hz, 1H), 7.02 (s, 1H), 6.98 (t, J = 7.5 Hz, 1H), 5.07 (s, 2H), 4.94 (dd, J = 7.8, 6.4 Hz, 1H), 4.18 (t, J = 6.4 Hz, 1H), 3.43 (dd, J = 14.6, 6.4 Hz, 1H), 3.36–3.31 (m, 1H), 2.81–2.73 (m, 2H), 2.30–2.20 (m, 2H) ppm; ^{13}C NMR (125 MHz, CD_3OD) δ 173.5, 169.4, 168.5, 142.3, 141.2, 138.1, 137.0, 130.9, 129.7, 129.7, 129.5, 129.5, 129.4, 129.4, 129.3, 129.3, 129.2, 129.2, 129.2, 128.7, 127.5, 124.5, 122.5, 120.5, 120.5, 119.9, 119.2, 112.4, 110.8, 68.0, 55.8, 55.2, 34.6, 32.0, 28.3 ppm; HRMS calcd for $C_{35}H_{35}N_4O_4$ [$M+H^+$] 575.2658 found 575.2669.

4.6.2.3. (S)-Methyl 2-(4-((S)-2-amino-5-guanidinopentanamido)benzamido)-3-(4-hydroxyphenyl)-propanoate (P23).

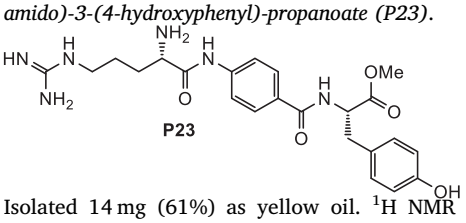

Isolated 14 mg (61%) as yellow oil. ^{1}H NMR (500 MHz, CD_3OD) δ 7.78–7.61 (m, 4H), 7.06 (d, J = 8.4 Hz, 2H), 6.70 (d, J = 8.4 Hz, 2H), 4.78–4.72 (m, 1H), 3.92–3.84 (m, 1H), 3.72 (s, 3H), 3.26–3.14 (m, 3H), 3.05–2.95 (m, 1H), 2.01–1.83 (m, 2H), 1.78–1.66 (m, 2H) ppm; ^{13}C NMR (125 MHz, CD_3OD) δ 173.9, 172.4, 169.4, 157.4, 156.6, 141.5, 131.2, 131.2, 129.5, 129.5, 129.4, 129.1, 120.5, 120.5, 116.3, 116.3, 56.2, 55.3, 52.7, 42.0, 37.5, 30.9, 25.7 ppm; HRMS calcd for $C_{23}H_{31}N_6O_5$ [$M+H^+$] 471.2356 found 471.2345.

4.6.2.4. (S)-Benzyl 2-(4-((S)-2-amino-4-(4-(benzyloxy)phenyl)butanamido)benzamido)-3-(1H-indol-3-yl)-propanoate (P24).

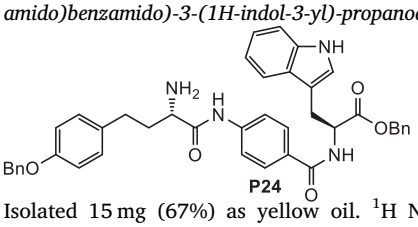

Isolated 15 mg (67%) as yellow oil. ^{1}H NMR (500 MHz, CD_3OD) δ 7.77–7.70 (m, 2H), 7.69–7.63 (m, 2H), 7.55 (d, J = 7.9 Hz, 1H), 7.41–7.23 (m, 9H), 7.22–7.05 (m, 5H), 7.03–6.97 (m, 2H), 6.90–6.82 (m, 2H), 5.12–5.03 (m, 2H), 4.98–4.89 (m, 3H), 4.15–4.05 (m, 1H), 3.48–3.34 (m, 2H), 2.77–2.61 (m, 2H), 2.29–2.15 (m, 2H) ppm; ^{13}C NMR (125 MHz, CD_3OD) δ 173.5, 172.9, 169.5, 159.4, 142.4, 138.7, 138.7, 138.1, 137.1, 131.5, 130.7, 129.7, 129.5, 129.4, 129.2, 129.2, 128.8, 128.5, 124.5, 122.5, 120.6, 119.9, 119.2, 116.3, 112.4, 110.9, 106.9, 71.1, 68.0, 57.8, 55.8, 43.8, 40.4, 28.3 ppm; HRMS calcd for $C_{42}H_{41}N_4O_5$ [$M+H^+$] 681.3077 found 681.3071.

4.6.2.5. (S)-2-(4-((S)-2-Aminohexanamido)benzamido)-3-(1H-indol-3-yl)-propanoic acid (P25).

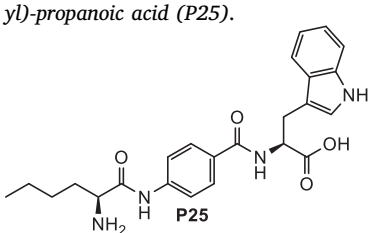

Isolated 11 mg (61%) as yellow oil. ^{1}H NMR (500 MHz, CD_3OD) δ 7.70–7.62 (m, 4H), 7.57 (d, J = 7.9 Hz, 1H), 7.30 (d, J = 7.9 Hz, 1H), 7.12 (s, 1H), 7.04 (t, J = 7.5 Hz, 1H), 6.92 (t, J = 7.4 Hz, 1H), 4.84–4.80 (m, 1H), 4.06–3.98 (m, 1H), 3.51–3.43 (m, 1H), 3.37–3.33 (m, 1H), 1.99–1.82 (m, 2H), 1.49–1.31 (m, 4H), 0.97–0.91 (m, 3H) ppm; ^{13}C NMR (125 MHz, CD_3OD) δ 177.4, 169.0, 168.8, 142.1, 138.0, 131.4, 129.3, 129.3, 129.2, 124.4, 122.2, 120.4, 120.4, 119.7, 119.5, 112.2, 111.7, 56.7, 55.3, 32.5, 28.6, 28.0, 23.4, 14.0 ppm; HRMS calcd for $C_{24}H_{29}N_4O_4$ [$M+H^+$] 437.2189 found 437.2177.

4.7. Synthesis of analogues P26-P30

The synthetic procedures are similar to the ones presented for analogues **P16**-**P20**. Specific equivalents and yields are reported in Scheme 5.

4.7.1. (S)-Benzyl 2-(2-((S)-2-aminohexanamido)isonicotinamido)-3-(1H-indol-3-yl)-propanoate (P26)

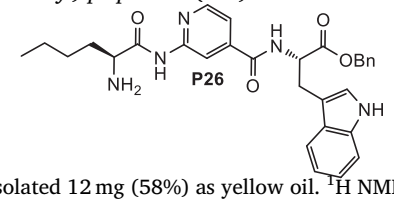

Isolated 12 mg (58%) as yellow oil. ^{1}H NMR (500 MHz, CD_3OD) δ 8.45 (d, J = 5.7 Hz, 1H), 8.16 (s, 1H), 7.62–7.58 (m, 1H), 7.54 (d, J = 7.9 Hz, 1H), 7.37–7.18 (m, 6H), 7.11–7.05 (m, 2H), 7.02–6.96 (m, 1H), 5.12 (s, 2H), 4.99–4.94 (m, 1H), 4.31–4.23 (m, 1H), 3.46 (dd, J = 14.6, 6.0 Hz, 1H), 3.38–3.33 (m, 1H), 2.10–1.95 (m, 2H), 1.54–1.38 (m, 4H), 0.96 (t, J = 6.9 Hz, 3H) ppm; ^{13}C NMR (125 MHz, CD_3OD) δ 172.9, 171.1, 166.3, 150.8, 149.0, 144.8, 138.0, 137.0, 129.5, 129.3, 129.2, 128.6, 124.7, 122.5, 119.9, 119.7, 119.1, 115.2, 112.5, 110.6, 68.2, 56.0, 55.3, 32.2, 28.2, 27.9, 23.4, 14.0 ppm; HRMS calcd for $C_{30}H_{34}N_5O_4$ [$M+H^+$] 528.2611 found 528.2603.

4.7.2. (S)-Benzyl 2-(2-((S)-2-amino-4-phenylbutanamido)isonicotinamido)-3-(1H-indol-3-yl)-propanoate (P27)

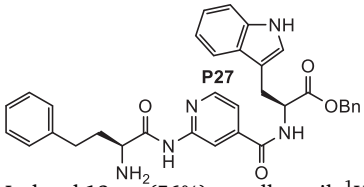

Isolated 13 mg (56%) as yellow oil. ^{1}H NMR (500 MHz, CD_3OD) δ 8.43 (d, J = 5.7 Hz, 1H), 8.09 (s, 1H), 7.62–7.56 (m, 1H), 7.55 (d, J = 7.9 Hz, 1H), 7.35–7.27 (m, 3H), 7.26–7.15 (m, 7H), 7.11–7.04 (m, 3H), 7.00 (t, J = 7.2 Hz, 1H), 5.13 (s, 2H), 5.01–4.93 (m, 1H), 4.40–4.32 (m, 1H), 3.47 (dd, J = 14.6, 6.0 Hz, 1H), 3.34 (dd, J = 14.6, 8.5 Hz, 1H), 2.83 (t, J = 8.1 Hz, 2H), 2.42–2.31 (m, 2H) ppm; ^{13}C NMR (125 MHz, CD_3OD) δ 172.9, 170.6, 166.3, 150.7, 148.9, 144.9, 140.9, 138.1, 137.0, 129.7, 129.7, 129.5, 129.5, 129.4, 129.4, 129.3, 129.2, 129.2, 128.7, 127.5, 124.7, 122.5, 119.9, 119.7, 119.1, 115.2, 112.5, 110.6, 68.2, 56.0, 55.2, 34.1, 31.8, 28.2 ppm; HRMS calcd for $C_{34}H_{34}N_5O_4$ [$M+H^+$] 576.2611 found 528.2623.

4.7.3. (S)-Methyl 6-amino-2-(2-((S)-2-amino-4-phenylbutanamido) isonicotinamido)-hexanoate (P28)

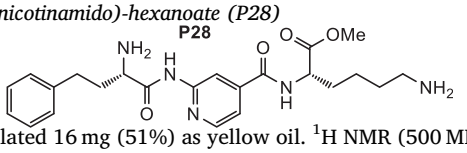

Isolated 16 mg (51%) as yellow oil. ^{1}H NMR (500 MHz, CD_3OD) δ 8.55 (d, J = 5.9 Hz, 1H), 8.19 (s, 1H), 7.90 (d, J = 5.7 Hz, 1H), 7.32–7.18 (m, 4H), 7.11 (t, J = 7.0 Hz, 1H), 4.65–4.60 (m, 1H), 4.52–4.30 (m, 1H), 3.77 (s, 3H), 2.97 (t, J = 7.3 Hz, 2H), 2.87 (t, J = 7.9 Hz, 2H), 2.49–2.31 (m, 2H), 2.08–1.87 (m, 2H), 1.82–1.69 (m, 2H), 1.65–1.49 (m, 2H) ppm; ^{13}C NMR (125 MHz, CD_3OD) δ 173.3, 171.3, 165.9, 150.1, 143.2, 143.2, 141.0, 129.6, 129.6, 129.5, 129.5, 127.5, 120.2, 115.9, 55.3, 54.6, 53.0, 40.5, 34.0, 31.8, 31.5, 28.0, 24.1 ppm; HRMS calcd for $C_{23}H_{32}N_5O_4$ [$M+H^+$] 442.2454 found 442.2445.

4.7.4. (S)-Benzyl 2-(2-((S)-2-aminohexanamido)isonicotinamido)-3-methylbutanoate (P29)

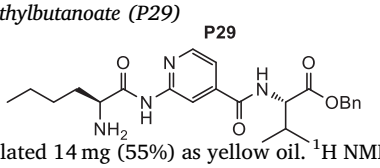

Isolated 14 mg (55%) as yellow oil. ^{1}H NMR (500 MHz, CD_3OD) δ 8.55 (d, J = 5.8 Hz, 1H), 8.26 (s, 1H), 7.78 (dd, J = 5.8, 1.5 Hz, 1H), 7.45–7.29 (m, 5H), 5.25 (d, J = 12.2 Hz, 1H), 5.18 (d, J = 12.2 Hz, 1H), 4.53 (d, J = 6.7 Hz, 1H), 4.28–4.20 (m, 1H), 2.36–2.24 (m, 1H), 2.12–1.94 (m, 2H), 1.54–1.39 (m, 4H), 1.06–0.94 (m, 9H) ppm; ^{13}C NMR (125 MHz, CD_3OD) δ 172.5, 170.9, 167.3, 151.2, 148.8, 145.8, 137.2, 129.6, 129.5, 129.4, 128.4, 119.8, 115.4, 115.1, 68.0, 60.6, 55.3, 32.2, 31.6, 27.9, 23.4, 19.6, 19.0, 14.0 ppm; HRMS calcd for $C_{24}H_{33}N_4O_4$ [$M+H^+$] 441.2502 found 441.2511.

4.7.5. (S)-Methyl 2-(2-((S)-2-aminohexanamido)isonicotinamido)-3-(4-hydroxyphenyl)-propanoate (P30)

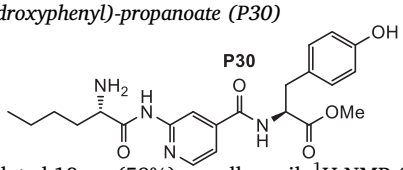

Isolated 18 mg (59%) as yellow oil. ^{1}H NMR (500 MHz, CD_3OD) δ 8.55 (dd, J = 6.2, 2.2 Hz, 1H), 8.05 (s, 1H), 7.78 (d, J = 6.1 Hz, 1H), 7.10 (dd, J = 12.0, 8.4 Hz, 2H), 6.71 (d, J = 8.2 Hz, 2H), 4.86–4.79 (m, 1H), 4.34–4.28 (m, 1H), 3.74 (s, 3H), 3.28–3.18 (m, 1H), 3.07–2.97 (m, 1H), 2.16–1.95 (m, 2H), 1.57–1.35 (m, 4H), 0.97 (t, J = 7.1 Hz, 3H) ppm; ^{13}C NMR (125 MHz, CD_3OD) δ 173.2, 170.9, 166.5, 157.4, 151.2, 148.6, 145.7, 131.2, 131.2, 128.8, 119.6, 116.4, 116.4, 114.9, 56.3, 55.3, 52.9, 37.3, 32.18, 27.9, 23.4, 14.0 ppm; HRMS calcd for $C_{22}H_{29}N_4O_5$ [$M+H^+$] 429.2138 found 429.2144.

4.8. Synthesis of analogues P31-P37

The synthetic procedures are similar to the ones presented for analogues **P16**-**P20**. Specific equivalents and yields are reported in Scheme 6.

4.8.1. (S)-Benzyl 2-(6-((S)-2-aminohexanamido)nicotinamido)-3-(1H-indol-3-yl)-propanoate (P31)

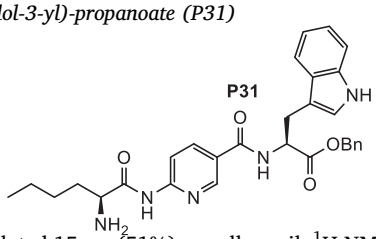

Isolated 15 mg (51%) as yellow oil. ^{1}H NMR (500 MHz, CD_3OD) δ 8.71 (s, 1H), 8.31 (d, J = 8.5 Hz, 1H), 8.04 (d, J = 8.2 Hz, 1H), 7.55 (d, J = 7.8 Hz, 1H), 7.38–7.25 (m, 4H), 7.25–7.17 (m, 2H), 7.12–7.02 (m, 2H), 6.99 (t, J = 7.5 Hz, 1H), 5.11 (s, 2H), 4.99–4.95 (m, 1H), 4.24–4.14 (m, 1H), 3.45 (dd, J = 14.6, 6.3 Hz, 1H), 3.40–3.31 (m, 1H), 2.10–1.86 (m, 2H), 1.52–1.38(m, 4H), 0.96 (t, J = 6.9 Hz, 3H) ppm; ^{13}C NMR (125 MHz, CD_3OD) δ 173.3, 170.4, 166.7, 153.2, 146.6, 140.9, 138.1, 137.0, 129.5, 129.5, 129.3, 129.3, 129.2, 128.7, 127.8, 124.5, 122.5, 119.9, 119.2, 115.3, 112.4, 110.7, 68.1, 55.9, 55.3, 32.2, 28.3, 27.9, 23.4, 14.0 ppm; HRMS calcd for $C_{30}H_{34}N_5O_4$ [$M+H^+$] 528.2611 found 528.2619.

4.8.2. (S)-Benzyl 2-(6-((S)-2-amino-4-phenylbutanamido)nicotinamido)-3-(1H-indol-3-yl)-propanoate (P32)

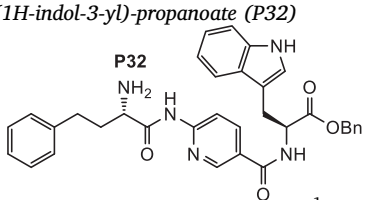

Isolated 15 mg (52%) as yellow oil. ^{1}H NMR (500 MHz, CD_3OD) δ 8.71 (s, 1H), 8.28 (d, J = 8.7 Hz, 1H), 8.07–7.85 (m, 1H), 7.56 (d, J = 7.9 Hz, 1H), 7.35 (d, J = 8.1 Hz, 1H), 7.33–7.19 (m, 9H), 7.17–7.06 (m, 3H), 7.00 (t, J = 7.4 Hz, 1H), 5.12 (s, 2H), 5.00–4.96 (m, 1H), 4.41–4.26 (m, 1H), 3.47 (dd, J = 14.4, 6.3 Hz, 1H), 3.22 (dd, J = 14.7, 7.3 Hz, 1H), 2.86–2.80 (m, 2H), 2.44–2.15 (m, 2H) ppm; ^{13}C NMR (125 MHz, CD_3OD) δ 173.3, 170.0, 166.7, 153.1, 146.5, 141.0, 140.8,

138.0, 137.0, 129.7, 129.7, 129.5, 129.5, 129.4, 129.4, 129.2, 129.2, 129.2, 128.7, 127.8, 127.5, 124.6, 122.5, 119.9, 119.1, 115.3, 112.5, 110.7, 68.1, 55.9, 55.2, 34.3, 31.9, 28.3 ppm; HRMS calcd for $C_{34}H_{34}N_5O_4$ [$M+H^+$] 576.2611 found 576.2617.

4.8.3. (S)-Methyl 2-(6-((S)-2-amino-5-guanidinopentanamido)nicotinamido)-3-(4-hydroxyphenyl)-propanoate (P33)

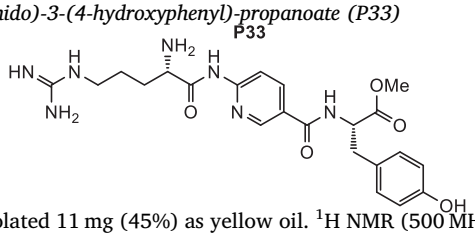

Isolated 11 mg (45%) as yellow oil. ^{1}H NMR (500 MHz, CD_3OD) δ 8.31 (s, 1H), 8.23 (dd, J = 9.3, 1.9 Hz, 1H), 7.12–7.03 (m, 3H), 6.70 (d, J = 8.4 Hz, 2H), 4.75 (dd, J = 9.3, 5.7 Hz, 1H), 4.04 (t, J = 6.3 Hz, 1H), 3.71 (s, 3H), 3.30–3.26 (m, 2H), 3.21–3.11 (m, 1H), 3.01 (dd, J = 13.9, 9.4 Hz, 1H), 2.09–1.91 (m, 2H), 1.89–1.67 (m, 2H) ppm; ^{13}C NMR (125 MHz, CD_3OD) δ 173.5, 171.4, 165.0, 158.7, 157.4, 156.5, 143.1, 137.8, 131.2, 131.2, 128.8, 120.5, 116.3, 116.3, 114.7, 56.2, 53.5, 41.7, 39.2, 37.3, 28.6, 25.7 ppm; HRMS calcd for $C_{22}H_{30}N_7O_5$ [$M+H^+$] 472.2308 found 472.2320.

4.8.4. (S)-Methyl 2-(6-((S)-2-amino-4-phenylbutanamido)nicotinamido)-3-(4-hydroxyphenyl)-propanoate (P34)

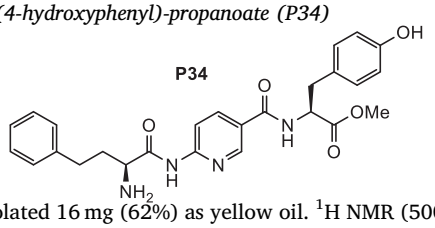

Isolated 16 mg (62%) as yellow oil. ^{1}H NMR (500 MHz, CD_3OD) δ 8.74 (s, 1H), 8.50 (d, J = 8.4 Hz, 1H), 7.92 (d, J = 8.4 Hz, 1H), 7.35–7.14 (m, 5H), 7.08 (d, J = 8.3 Hz, 2H), 6.71 (d, J = 8.3 Hz, 2H), 4.84–4.78 (m, 1H), 4.48–4.38 (m, 1H), 3.72 (s, 3H), 3.25–3.16 (m, 1H), 3.09–2.99 (m, 1H), 2.90–2.82 (m, 2H), 2.46–2.30 (m, 2H) ppm; ^{13}C NMR (125 MHz, CD_3OD) δ 173.4, 171.0, 165.2, 157.4, 151.4, 143.4, 143.3, 140.9, 131.2, 131.2, 129.6, 129.6, 129.4, 129.4, 128.8, 128.2, 127.4, 116.6, 116.3, 116.3, 56.3, 55.2, 52.9, 37.3, 34.0, 31.7 ppm; HRMS calcd for $C_{26}H_{29}N_4O_5$ [$M+H^+$] 477.2138 found 477.2151.

4.8.5. (S)-Benzyl 2-(6-((S)-2-amino-3-(4-(benzyloxy)phenyl)propanamido)nicotinamido)-3-(1H-indol-3-yl)-propanoate (P35)

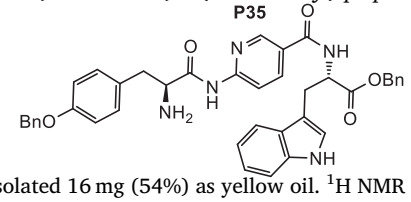

Isolated 16 mg (54%) as yellow oil. ^{1}H NMR (500 MHz, CD_3OD) δ 8.68 (s, 1H), 8.23 (d, J = 8.1 Hz, 1H), 8.03 (d, J = 7.7 Hz, 1H), 7.55 (d, J = 7.9 Hz, 1H), 7.45–7.15 (m, 13H), 7.13–6.90 (m, 5H), 5.11 (s, 2H), 5.04 (s, 2H), 4.99–4.94 (m, 1H), 4.43–4.29 (m, 1H), 3.49–3.41 (m, 1H), 3.37–3.33 (m, 2H), 3.17–3.07 (m, 1H) ppm; ^{13}C NMR (125 MHz, CD_3OD) δ 173.3, 169.7, 166.9, 160.0, 153.3, 147.0, 140.5, 138.6, 138.1, 137.0, 131.7, 131.7, 131.7, 129.5, 129.5, 129.5, 129.3, 129.2, 128.9, 128.7, 128.5, 127.8, 127.1, 124.5, 122.5, 119.9, 119.1, 116.6, 116.6, 116.6, 116.4, 115.1, 112.5, 110.8, 70.9, 68.1, 56.5, 55.9, 37.6, 28.3 ppm; HRMS calcd for $C_{40}H_{38}N_5O_5$ [$M+H^+$] 668.2873 found 668.2875.

4.8.6. (S)-Methyl 2-(6-((S)-2-aminohexanamido)nicotinamido)-3-(4-hydroxyphenyl)-propanoate (P36)

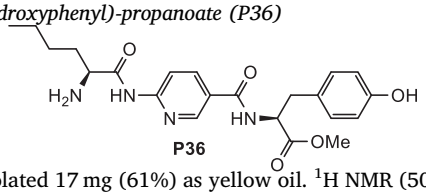

Isolated 17 mg (61%) as yellow oil. ^{1}H NMR (500 MHz, CD_3OD) δ 8.71 (s, 1H), 8.25 (dd, J = 8.7, 2.2 Hz, 1H), 8.17–8.07 (m, 1H), 7.12–7.05 (m, 2H), 6.70 (d, J = 8.5 Hz, 2H), 4.82–4.76 (m, 1H), 4.14 (bs, 1H), 3.90–3.86 (m, 1H), 3.73 (s, 3H), 3.25–3.15 (m, 1H), 3.05–2.97 (m, 1H), 2.09–1.83 (m, 2H), 1.53–1.39 (m, 4H), 0.96 (t, J = 7.0 Hz, 3H) ppm; ^{13}C NMR (125 MHz, CD_3OD) δ 173.6, 170.9, 162.0, 153.4, 147.5, 140.8, 140.2, 131.2, 131.2, 128.9, 116.3, 116.3, 115.1, 114.2, 56.2, 55.3, 52.8, 37.4, 32.3, 27.9, 23.4, 14.0 ppm; HRMS calcd for $C_{22}H_{29}N_4O_5$ [$M+H^+$] 429.2138 found 429.2125.

4.8.7. (S)-2-(6-((S)-2-Aminohexanamido)nicotinamido)-3-(1H-indol-3-yl)-propanoic acid (P37)

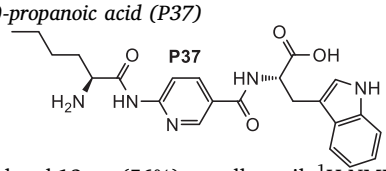

Isolated 12 mg (56%) as yellow oil. ^{1}H NMR (500 MHz, CD_3OD) δ 8.69 (s, 1H), 8.33 (dd, J = 8.8, 2.1 Hz, 1H), 8.00 (d, J = 9.0 Hz, 1H), 7.58 (d, J = 7.9 Hz, 1H), 7.32 (d, J = 7.9 Hz, 1H), 7.15 (s, 1H), 7.07 (t, J = 7.6 Hz, 1H), 6.98 (t, J = 7.6 Hz, 1H), 4.97–4.92 (m, 1H), 4.23–4.16 (m, 1H), 3.54–3.46 (m, 1H), 3.36–3.32 (m, 1H), 2.11–1.84 (m, 2H), 1.54–1.27 (m, 4H), 0.96 (t, J = 6.9 Hz, 6H) ppm; ^{13}C NMR (125 MHz, CD_3OD) δ 173.9, 170.2, 166.9, 153.6, 147.2, 140.4, 138.1, 128.7, 127.8, 124.4, 122.5, 119.9, 119.1, 115.1, 112.4, 110.9, 55.7, 55.3, 32.3, 28.3, 27.9, 23.4, 14.0 ppm; HRMS calcd for $C_{23}H_{28}N_5O_4$ [$M+H^+$] 438.2141 found 438.2147.

4.9. Synthesis of analogues P38-P44

The synthetic procedures are similar to the ones presented for analogues **P16**-**P20**. Specific equivalents and yields are reported in Scheme 7.

4.9.1. (S)-Benzyl 2-(3-(2-((S)-2-aminohexanoyl)hydrazinyl)benzamido)-3-(1H-indol-3-yl)-propanoate (P38)

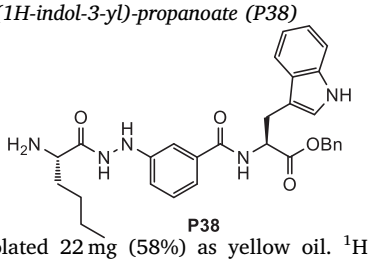

Isolated 22 mg (58%) as yellow oil. ^{1}H NMR (500 MHz, CD_3OD) δ 7.58–7.52 (m, 1H), 7.37–7.30 (m, 1H), 7.31–7.14 (m, 8H), 7.13–7.06 (m, 1H), 7.04–6.95 (m, 3H), 5.12–5.05 (m, 2H), 4.96–4.90 (m, 1H), 4.03–3.94 (m, 1H), 3.48–3.38 (m, 1H), 3.36–3.32 (m, 1H), 2.03–1.83 (m, 2H), 1.54–1.33 (m, 4H), 1.01–0.86 (m, 3H) ppm; ^{13}C NMR (125 MHz, CD_3OD) δ 173.5, 170.6, 170.3, 149.9, 138.1, 137.0, 136.0, 130.2, 129.5, 129.5, 129.2, 129.1, 128.7, 124.5, 122.5, 120.0, 119.9, 119.8, 119.2, 117.6, 112.9, 112.4, 110.7, 68.0, 55.7, 53.4, 32.4, 28.3, 27.9, 23.3, 14.1 ppm; HRMS calcd for $C_{31}H_{36}N_5O_4$ [$M+H^+$] 542.2767 found 542.2781.

4.9.2. (S)-Benzyl 2-(3-(2-((S)-2-amino-4-phenylbutanoyl)hydrazinyl) benzamido)-3-(1H-indol-3-yl)-propanoate (P39)

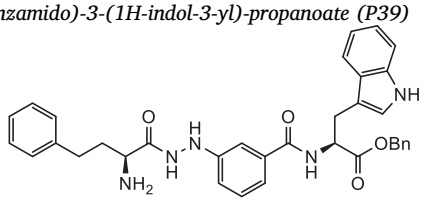

P39

Isolated 28 mg (56%) as yellow oil. ^{1}H NMR (500 MHz, CD_3OD) δ 7.54 (d, J = 8.0 Hz, 1H), 7.34 (d, J = 8.0 Hz, 1H), 7.30–7.11 (m, 12H), 7.12–7.05 (m, 2H), 7.03–6.94 (m, 3H), 5.06 (s, 2H), 4.97–4.89 (m, 1H), 4.07 (t, J = 6.4 Hz, 1H), 3.48–3.37 (m, 1H), 3.35–3.29 (m, 1H), 2.85–2.63 (m, 2H), 2.27–2.15 (m, 2H) ppm; ^{13}C NMR (125 MHz, CD_3OD) δ 173.5, 170.3, 170.3, 165.5, 149.9, 145.6, 141.2, 138.1, 136.1, 130.2, 129.7, 129.7, 129.5, 129.5, 129.3, 129.3, 129.1, 129.1, 128.7, 127.6, 124.5, 122.5, 119.9, 119.8, 119.2, 117.7, 112.9, 112.4, 110.7, 68.0, 55.7, 53.3, 34.7, 32.0, 28.3 ppm; HRMS calcd for $C_{35}H_{36}N_5O_4$ [$M+H^+$] 590.2767 found 590.2765.

4.9.3. (S)-Methyl 6-amino-2-(3-(2-((S)-2-amino-4-phenylbutanoyl) hydrazinyl)benzamido)-hexanoate (P40)

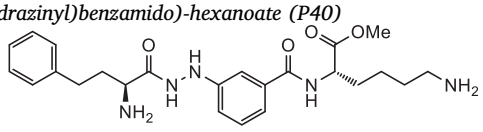

P40

Isolated 26 mg (53%) as yellow oil. ^{1}H NMR (500 MHz, CD_3OD) δ 7.41–7.33 (m, 2H), 7.33–7.24 (m, 4H), 7.21 (t, J = 6.3 Hz, 1H), 7.16–7.10 (m, 1H), 7.08–7.04 (m, 1H), 4.60–4.54 (m, 1H), 4.20–4.14 (m, 1H), 3.71 (s, 3H), 2.96–2.88 (m, 2H), 2.84–2.72 (m, 2H), 2.30–2.20 (m, 2H), 2.01–1.87 (m, 2H), 1.78–1.68 (m, 2H), 1.61–1.41 (m, 2H) ppm; ^{13}C NMR (125 MHz, CD_3OD) δ 174.0, 170.6, 170.5, 149.9, 141.4, 135.9, 130.3, 129.7, 129.7, 129.4, 129.4, 127.5, 120.2, 117.7, 113.0, 54.3, 53.3, 52.8, 40.5, 34.7, 32.1, 31.5, 28.0, 24.1 ppm; HRMS calcd for $C_{24}H_{34}N_5O_4$ [$M+H^+$] 456.2611 found 456.2622.

4.9.4. (S)-Benzyl 2-(3-(2-((S)-2-aminohexanoyl)hydrazinyl)benzamido)-3-methylbutanoate (P41)

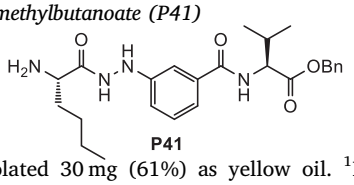

P41

Isolated 30 mg (61%) as yellow oil. ^{1}H NMR (500 MHz, CD_3OD) δ 7.40–7.24 (m, 8H), 7.04–7.00 (m, 1H), 5.23 (d, J = 12.2 Hz, 1H), 5.16 (d, J = 12.2 Hz, 1H), 4.49 (d, J = 6.9 Hz, 1H), 3.98 (t, J = 6.4 Hz, 1H), 2.31–2.21 (m, 1H), 2.02–1.86 (m, 2H), 1.50–1.38 (m, 4H), 1.03–0.93 (m, 9H) ppm; ^{13}C NMR (125 MHz, CD_3OD) δ 173.1, 170.9, 170.7, 150.0, 137.2, 136.3, 130.2, 129.6, 129.6, 129.4, 129.4, 129.3, 119.9, 117.6, 113.0, 67.8, 60.3, 53.4, 32.5, 31.7, 28.0, 23.4, 19.6, 19.1, 14.1 ppm; HRMS calcd for $C_{25}H_{35}N_4O_4$ [$M+H^+$] 455.2658 found 455.2656.

4.9.5. (S)-Methyl 2-(3-(2-((S)-2-aminohexanoyl)ydrazinyl) benzamido)-3-(4-hydroxy phenyl)-propanoate (P42)

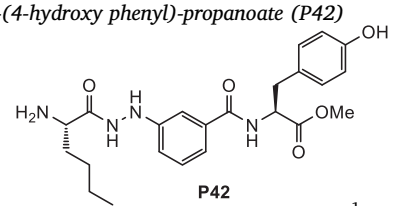

P42

Isolated 25 mg (61%) as yellow oil. ^{1}H NMR (500 MHz, CD_3OD) δ 7.29–7.24 (m, 1H), 7.23–7.17 (m, 2H), 7.09–7.02 (m, 2H), 7.02–6.96 (m, 1H), 6.73–6.68 (m, 2H), 4.79–4.72 (m, 1H), 4.02–3.91 (m, 1H), 3.71 (s, 3H), 3.21–3.11 (m, 1H), 3.06–2.99 (m, 1H), 2.03–1.77 (m, 2H), 1.49–1.37 (m, 4H), 0.97 (t, J = 6.8 Hz, 3H) ppm; ^{13}C NMR (125 MHz, CD_3OD) δ 173.8, 170.7, 170.3, 157.3, 149.9, 136.1, 131.2, 131.2, 130.2, 129.0, 119.7, 117.6, 116.3, 116.3, 112.9, 56.2, 53.4, 52.7, 37.4, 32.4, 28.0, 23.3, 14.1 ppm; HRMS calcd for $C_{23}H_{31}N_4O_5$ [$M+H^+$] 443.2294 found 443.2289.

4.9.6. (S)-Methyl 2-(3-(2-((S)-2-amino-5-guanidinopentanoyl)hydrazinyl) benzamido)-3-(4-hydroxyphenyl)-propanoate (P43)

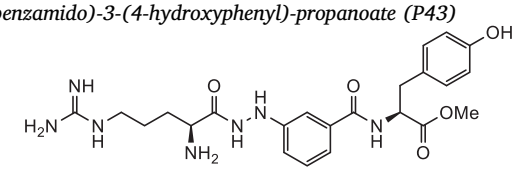

P43

Isolated 19 mg (51%) as yellow oil. ^{1}H NMR (500 MHz, CD_3OD) δ 7.75–7.72 (m, 1H), 7.48–7.40 (m, 1H), 7.33–7.17 (m, 2H), 7.14–7.01 (m, 2H), 6.71 (d, J = 8.4 Hz, 2H), 4.86–4.68 (m, 1H), 4.16–4.04 (m, 1H), 3.72 (s, 3H), 3.31–3.25 (m, 2H), 3.24–3.14 (m, 1H), 3.06–3.02 (m, 1H), 2.15–1.93 (m, 2H), 1.89–1.61 (m, 2H) ppm; ^{13}C NMR (125 MHz, CD_3OD) δ 173.8, 173.7, 170.6, 170.3, 158.7, 157.3, 132.8, 131.2, 131.2, 129.5, 129.1, 128.4, 116.3, 116.3, 56.2, 53.6, 52.8, 41.7, 37.4, 28.6, 25.7 ppm; HRMS calcd for $C_{23}H_{32}N_7O_5$ [$M+H^+$] 486.2465 found 486.2479.

4.9.7. (S)-2-(3-(2-((S)-2-Amino-5-guanidinopentanoyl)hydrazinyl) benzamido)-3-(1H-indol-3-yl)-propanoic acid (P44)

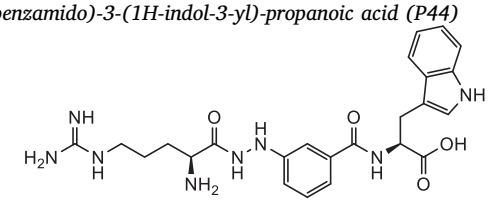

P44

Isolated 21 mg (53%) as yellow oil. ^{1}H NMR (500 MHz, CD_3OD) δ 7.71–6.90 (m, 9H), 4.13–4.09 (m, 1H), 3.56–3.43 (m, 1H), 3.37–3.32 (m, 1H), 3.21 –3.12 (m, 1H), 3.04–2.92 (m, 1H), 2.90–2.75 (m, 1H), 1.78–1.55 (m, 3H), 1.38–1.28 (m, 1H) ppm; ^{13}C NMR (125 MHz, CD_3OD) δ 175.3, 170.6, 166.6, 158.8, 158.7, 132.8, 132.7, 132.6, 129.5, 128.4, 124.5, 124.4, 123.5, 122.4, 119.8, 119.2, 112.4, 112.3, 53.8, 53.6, 41.7, 28.7, 28.2, 25.7 ppm; HRMS calcd for $C_{24}H_{31}N_8O_4$ [$M+H^+$] 495.2468 found 495.2453.

4.10. Synthesis of analogues P45-P49

The synthetic procedures are similar to the ones presented for analogues **P16**-**P20**. Specific equivalents and yields are reported in Scheme 8.

4.10.1. (S)-Benzyl 2-(4-(2-((S)-2-aminohexanoyl)hydrazinyl)benzamido)-3-(1H-indol-3-yl)-propanoate (P45)

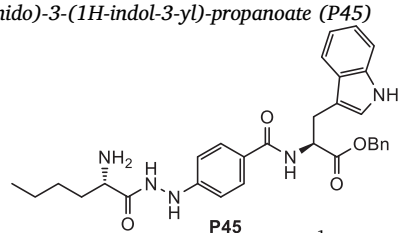

P45

Isolated 25 mg (63%) as yellow oil. ^{1}H NMR (500 MHz, CD_3OD) δ 7.65 (d, J = 8.7 Hz, 2H), 7.55 (d, J = 7.9 Hz, 1H), 7.34 (d, J = 8.1 Hz, 2H), 7.30–7.24 (m, 3H), 7.22–7.14 (m, 2H), 7.12–7.06 (m, 1H), 7.03–6.96 (m, 2H), 6.81 (d, J = 8.7 Hz, 1H), 5.08 (s, 2H), 4.94–4.91 (m, 1H), 4.04–3.96 (m, 1H), 3.45–3.38 (m, 1H), 3.34–3.30 (m, 1H), 2.17–1.84 (m, 2H), 1.60–1.39 (m, 4H), 0.99 (t, J = 6.9 Hz, 3H) ppm; ^{13}C NMR (125 MHz, CD_3OD) δ 173.7, 170.6, 169.9, 152.8, 138.1, 137.1, 130.2, 130.0, 130.0, 129.4, 129.4, 129.2, 129.2, 128.8, 125.9, 124.5, 122.5, 119.9, 119.2, 113.2, 112.9, 112.4, 110.8, 67.9, 55.7, 53.4, 32.4, 28.3,

27.9, 23.4, 14.1 ppm; HRMS calcd for $C_{31}H_{36}N_5O_4$ [$M+H^+$] 542.2767 found 542.2781.

4.10.2. (S)-Benzyl 2-(4-(2-((S)-2-amino-4-phenylbutanoyl)hydrazinyl) benzamido)-3-(1H-indol-3-yl)-propanoate (P46)

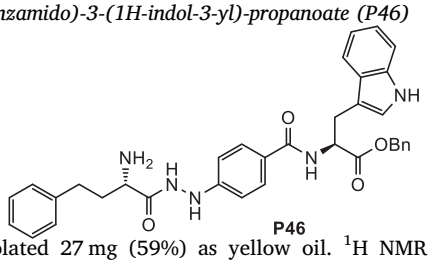

P46

Isolated 27 mg (59%) as yellow oil. ^{1}H NMR (500 MHz, CD_3OD) δ 7.67–7.61 (m, 2H), 7.57–7.51 (m, 1H), 7.37–7.12 (m,11*H*), 7.10–7.05 (m, 2H), 7.02–6.94 (m, 1H), 6.82–6.77 (m, 2H), 5.06 (s, 2H), 4.94–4.90 (m, 1H), 3.69–3.63 (m, 1H), 3.55–3.47 (m, 1H), 3.43–3.35 (m, 1H), 2.75–2.67 (m, 2H), 2.11–2.01 (m, 1H), 1.98–1.89 (m, 1H) ppm; ^{13}C NMR (125 MHz, CD_3OD) δ 176.5, 173.8, 169.9, 153.2, 142.6, 138.0, 137.1, 129.9, 129.9, 129.6, 129.6, 129.5, 129.5, 129.4, 129.4, 129.2, 129.2, 128.8, 127.1, 125.7, 125.6, 124.5, 122.5, 119.9, 119.2, 112.8, 112.8, 112.4, 110.8, 67.9, 55.7, 54.4, 38.1, 32.8, 28.3 ppm; HRMS calcd for $C_{35}H_{36}N_5O_4$ [$M+H^+$] 590.2767 found 590.2757.

4.10.3. (S)-Methyl 2-(4-(2-((S)-2-amino-5-guanidinopentanoyl)hydrazinyl)benzamido)-3-(4-hydroxyphenyl)-propanoate (P47)

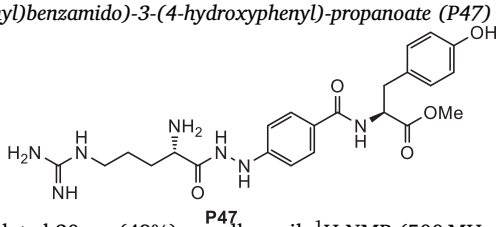

P47

Isolated 20 mg (48%) as yellow oil. ^{1}H NMR (500 MHz, CD_3OD) δ 7.73 (d, J = 7.3 Hz, 2H), 7.46–7.40 (m, 2H), 7.07 (d, J = 8.4 Hz, 2H), 6.74–6.67 (m, 2H), 4.82–4.71 (m, 1H), 4.15–4.09 (m, 1H) 3.72 (s, 3H), 3.29–3.24 (m, 2H), 3.18 (dd, J = 13.8, 5.7 Hz, 1H), 3.03 (dd, J = 13.8, 9.2 Hz, 1H), 2.13–1.88 (m, 2H), 1.87–1.61 (m, 2H) ppm; ^{13}C NMR (125 MHz, CD_3OD) δ 173.8, 170.6, 170.3, 159.1, 158.7, 157.4, 135.2, 132.8, 132.8, 131.2, 131.2, 129.5, 129.1, 128.4, 116.3, 116.3, 56.2, 53.6, 52.7, 41.7, 37.4, 28.7, 25.7 ppm; HRMS calcd for $C_{23}H_{32}N_7O_5$ [$M+H^+$] 486.2465 found 486.2464.

4.10.4. (S)-Methyl 2-(4-(2-((S)-2-amino-4-phenylbutanoyl)hydrazinyl) benzamido)-3-(4-hydroxyphenyl)-propanoate (P48)

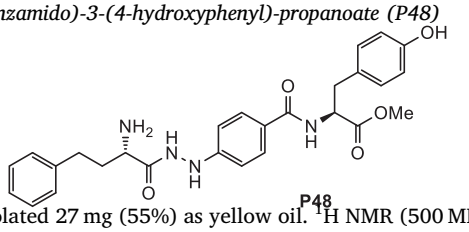

P48

Isolated 27 mg (55%) as yellow oil. ^{1}H NMR (500 MHz, CD_3OD) δ 7.66 (d, J = 8.1 Hz, 2H), 7.37–7.17 (m, 5H), 7.10–7.01 (m, 2H), 6.85 (d, J = 8.0 Hz, 2H), 6.73–6.67 (m, 2H), 4.77–4.70 (m, 1H), 4.15–4.09 (m, 1H), 3.70 (s, 3H), 3.21–3.10 (m, 1H), 3.07–2.96 (m, 1H), 2.85–2.75 (m, 2H), 2.29–2.14 (m, 2H) ppm; ^{13}C NMR (125 MHz, CD_3OD) δ 174.0, 170.3, 169.8, 157.3, 152.8, 141.2, 131.2, 131.2, 130.2, 129.9, 129.8, 129.6, 129.3, 129.1, 127.6, 125.9, 116.3, 116.3, 113.8, 113.2, 112.9, 56.1, 53.3, 52.7, 37.4, 34.7, 32.0 ppm; HRMS calcd for $C_{27}H_{31}N_4O_5$ [$M+H^+$] 491.2294 found 491.2302.

4.10.5. (S)-Methyl 2-(4-(2-((S)-2-aminohexanoyl)hydrazinyl)benzamido)-3-(4-hydroxyphenyl)-propanoate (P49)

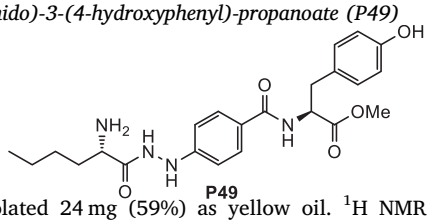

P49

Isolated 24 mg (59%) as yellow oil. ^{1}H NMR (500 MHz, CD_3OD) δ 7.68–7.62 (m, 2H), 7.09–7.03 (m, 2H), 6.83 (dd, J = 8.8, 2.1 Hz, 2H), 6.69 (dd, J = 8.5, 2.9 Hz, 2H), 4.79–4.70 (m, 1H), 4.00 (t, J = 6.4 Hz, 1H), 3.70 (s, 3H), 3.25–3.11 (m, 1H), 3.08–2.98 (m, 1H), 2.03–1.85 (m, 2H), 1.53–1.36 (m, 4H), 0.99 (t, J = 6.9 Hz, 3H) ppm; ^{13}C NMR (125 MHz, CD_3OD) δ 175.2, 174.1, 169.8, 157.3, 152.8, 131.3, 131.2, 129.9, 129.9, 129.3, 129.1, 116.3, 116.2, 113.2, 112.9, 56.1, 55.8, 53.4, 37.5, 32.4, 27.9, 23.4, 14.1 ppm; HRMS calcd for $C_{23}H_{31}N_4O_5$ [$M+H^+$] 443.2294 found 443.2306.

4.11. Biochemical methods

Recombinant proteins and assay utilized for evaluating *in vitro* inhibitor efficacy have been performed as described previously.[8c] The following enzyme concentrations were used for the inhibition and Michaelis-Menten assays: ERAP1, 10 nM; ERAP2, 2 nM; IRAP 1 nM. K_i values for competitive inhibition were calculated using K_M values for L-AMC for ERAP1, 546 μM, for R-AMC for ERAP2, 60 μM and for L-AMC for IRAP, 55μM, as described before.[17] Michaelis-Menten analysis was performed as described before.[18] The IC_{50} values of the MMP-12 inhibitors was measured using the OmniMMP fluorogenic substrate (Enzo Life Science, Farmingdale, NY, USA), by evaluating the ability of the compounds to prevent hydrolysis of the fluorescent-quenched peptide. The assay was carried out in a 50 mM HEPES buffer solution pH 7.5, 10 mM $CaCl_2$, 0.05% Brij-35 using 1 nM of enzyme and 1 mM of substrate in the absence of AHA. The measurements were performed with a Cary Eclipse spectrophotometer equipped with a plate reader following the increase in fluorescence induced by the hydrolysis of the substrate (excitation at 328 nm; emission at 393 nm).

Acknowledgments

We acknowledge support of this work by the projects “Development of Materials and Devices for Industrial, Health, Environmental and Cultural Applications” (MIS 5002567) and “NCSRD – INRASTES” research activities in the framework of the national RIS3“ (MIS 5002559) which are implemented under the “Action for the Strategic Development on the Research and Technological Sector”, funded by the Operational Programme ”Competitiveness, Entrepreneurship and Innovation“ (NSRF 2014-2020) and co-financed by Greece and the European Union (European Regional Development Fund).

Appendix A. Supplementary material

Supplementary data to this article can be found online at https://doi.org/10.1016/j.bmc.2019.115177.

References

1. Amin SA, Adhikari N, Jha T. Design of aminopeptidase n inhibitors as anti-cancer agents. *J Med Chem.* 2018;61:6468–6490.
2. Evnouchidou I, Papakyriakou A, Stratikos E. A new role for zn(ii) aminopeptidases: antigenic peptide generation and destruction. *Curr Pharm Des.* 2009;15:3656–3670.
3. Tsujimoto M, Hattori A. The oxytocinase subfamily of m1 aminopeptidases. *Biochim Biophys Acta.* 2005;1751:9–18.

4. a) Weimershaus M, Evnouchidou I, Saveanu L, van Endert P. Peptidases trimming mhc class i ligands. *Curr Opin Immunol.* 2012;25:90–96;

   b) Papakyriakou A, Stratikos E. The role of conformational dynamics in antigen trimming by intracellular aminopeptidases. *Front Immunol.* 2017;8:946.
5. a) Stratikos E. Regulating adaptive immune responses using small molecule modulators of aminopeptidases that process antigenic peptides. *Curr Opin Chem Biol.* 2014;23C:1–7;

   b) Georgiadis D, Mpakali A, Koumantou D, Stratikos E. Inhibitors of er aminopeptidase 1 and 2: from design to clinical application. *Curr Med Chem.* 2018;25:1. https://doi.org/10.2174/0929867325666180214111849.
6. a) Hattori A, Tsujimoto M. Endoplasmic reticulum aminopeptidases: Biochemistry, physiology and pathology. *J Biochem.* 2013;154:219–228;

   b) Hallberg M. Targeting the insulin-regulated aminopeptidase/at4 receptor for cognitive disorders. *Drug News Perspect.* 2009;22:133–139;

   c) Hisatsune C, Ebisui E, Usui M, et al. Erp44 exerts redox-dependent control of blood pressure at the er. *Mol Cell.* 2015;58:1015–1027;

   d) Goto Y, Ogawa K, Nakamura TJ, Hattori A, Tsujimoto M. Tlr-mediated secretion of endoplasmic reticulum aminopeptidase 1 from macrophages. *J Immunol.* 2014;192:4443–4452.
7. Diwakarla S, Nylander E, Gronbladh A, et al. Aryl sulfonamide inhibitors of insulin-regulated aminopeptidase enhance spine density in primary hippocampal neuron cultures. *ACS Chem Neurosci.* 2016;7:1383–1392.
8. a) Mpakali A, Giastas P, Deprez-Poulain R, et al. Crystal structures of erap2 complexed with inhibitors reveal pharmacophore requirements for optimizing inhibitor potency. *ACS Med Chem Lett.* 2017;8:333–337;

   b) Papakyriakou A, Zervoudi E, Theodorakis EA, Saveanu L, Stratikos E, Vourloumis D. Novel selective inhibitors of aminopeptidases that generate antigenic peptides. *Bioorg Med Chem Lett.* 2013;23:4832–4836;

   c) Papakyriakou A, Zervoudi E, Tsoukalidou S, et al. 3,4-diaminobenzoic acid derivatives as inhibitors of the oxytocinase subfamily of m1 aminopeptidases with immune-regulating properties. *J Med Chem.* 2015;58:1524–1543.
9. a) Jacobsen FE, Lewis JA, Cohen SM. A new role for old ligands: Discerning chelators for zinc metalloproteinases. *J Am Chem Soc.* 2006;128:3156–3157;

   b) Jacobsen JA, Major Jourden JL, Miller MT, Cohen SM. To bind zinc or not to bind zinc: An examination of innovative approaches to improved metalloproteinase inhibition. *Biochim Biophys Acta Mol Cell Res.* 2010;1803:72–94;

   c) Puerta DT, Cohen SM. Examination of novel zinc-binding groups for use in matrix metalloproteinase inhibitors. *Inorg Chem.* 2003;42:3423–3430;

   d) Puerta DT, Griffin MO, Lewis JA, et al. Heterocyclic zinc-binding groups for use in next-generation matrix metalloproteinase inhibitors: Potency, toxicity, and reactivity. *J Biol Inorg Chem.* 2006;11:131–138;

   e) Puerta DT, Lewis JA, Cohen SM. New beginnings for matrix metalloproteinase inhibitors: Identification of high-affinity zinc-binding groups. *J Am Chem Soc.* 2004;126:8388–8389.
10. Patil V, Sodji QH, Kornacki JR, Mrksich M, Oyelere AK. 3-hydroxypyridin-2-thione as novel zinc binding group for selective histone deacetylase inhibition. *J Med Chem.* 2013;56:3492–3506.
11. Giastas P, Neu M, Rowland P, Stratikos E. High-resolution crystal structure of endoplasmic reticulum aminopeptidase 1 with bound phosphinic transition-state analogue inhibitor. *ACS Med Chem Lett.* 2019;10:708–713.
12. Streater M, Taylor PD, Hider RC, Porter J. Novel 3-hydroxy-2(1h)-pyridinones. Synthesis, iron(iii)-chelating properties, and biological activity. *J Med Chem.* 1990;33:1749–1755.
13. Hanessian S, Saavedra OM, Mascitti V, Marterer W, Oehrlein R, Mak CP. Practical syntheses of b disaccharide and linear b type 2 trisaccharide - non-primate epitope markers recognized by human anti-α-gal antibodies causing hyperacute rejection of xenotransplants. *Tetrahedron.* 2001;57:3267–3280.
14. Jesberger M, Davis TP, Barner L. Applications of lawesson's reagent in organic and organometallic syntheses. *Synthesis.* 2003;1929–1958.
15. Bertini I, Calderone V, Cosenza M, et al. Conformational variability of matrix metalloproteinases: beyond a single 3d structure. *Proc Natl Acad Sci USA.* 2005;102:5334–5339.
16. Mannino C, Nievo M, Machetti F, et al. Synthesis of bicyclic molecular scaffolds (btaa): an investigation towards new selective mmp-12 inhibitors. *Bioorg Med Chem.* 2006;14:7392–7403.
17. Cer RZ, Mudunuri U, Stephens R, Lebeda FJ. Ic50-to-ki: a web-based tool for converting ic50 to ki values for inhibitors of enzyme activity and ligand binding. *Nucl Acids Res.* 2009;37:W441–445.
18. Stamogiannos A, Maben Z, Papakyriakou A, et al. Critical role of interdomain interactions in the conformational change and catalytic mechanism of endoplasmic reticulum aminopeptidase 1. *Biochemistry.* 2017;56:1546–1558.